Mycobacterium tuberculosis growth arrest on propionate at acidic pH is suppressed by mutations in *phoPR* and pyrazinamide treatment

Heather M. Murdoch[1,2], Shelby J. Dechow[1,2], Bassel J. Abdalla[1] and Robert B. Abramovitch[1*].

[1]Department of Microbiology, Genetics & Immunology, Michigan State University, East Lansing, MI,48824

[2]Co-first authors contributed equally to this study.

Disclosures

R.B.A. is an owner of Tarn Biosciences, Inc., a company that is working to develop new antimycobacterial drugs.

***Corresponding Author:**

Robert B. Abramovitch

E-mail: abramov5@msu.edu

Phone: (517) 884-5416

Fax: (517) 353-8957

Abstract

Mycobacterium tuberculosis (Mtb) arrests its growth at acidic pH, when grown on specific single carbon sources, including propionate. However, Mtb grows well on propionate at pH 7.0, supporting that propionate can support growth as a sole carbon source. To understand the basis of the propionate-driven growth arrest at acidic pH, we performed a forward genetic selection for mutants that enable growth on propionate at pH 5.7. All the selected mutants had insertions in the two-component regulatory genes *phoR* or *phoP*. We hypothesized that growth arrest at acidic pH is caused by PhoPR diverting carbon from central carbon metabolism towards lipid anabolism and that when PhoPR is inactivated, growth is promoted through metabolizing propionate by the methyl citrate cycle (MCC) into pyruvate, a permissive carbon source for growth at acidic pH. Using chemical inhibition and mutants of the MCC pathway, we demonstrate that the enhanced growth is dependent on the MCC. Furthermore, stimulating lipid synthesis via the methylmalonyl-CoA pathway by adding vitamin B12 restricts growth in the *ΔphoPR* mutant and, conversely, restricting lipid anabolism by inhibiting the triacylglycerol (TAG) synthase *tgs1* enhances growth of the *ΔphoPR* mutant. Notably, CoA pools increased in the *ΔphoPR* mutant grown on propionate, directly supporting our model. Given the role of CoA metabolism in pyrazinamide sensitivity, we examined Mtb sensitivity to pyrazinamide on propionate at acidic pH and, surprisingly, observed that pyrazinamide treatment of WT Mtb suppresses growth arrest on propionate at acidic pH. In contrast, the *phoPR* mutant has enhanced sensitivity to pyrazinamide. Together, these findings support that propionate-driven growth arrest at acidic pH is caused by metabolic remodeling that is regulated by PhoPR and is associated with pyrazinamide sensitivity.

Importance

When grown on certain single carbon sources, such as propionate, Mtb arrests its growth at acidic pH and establishes a state of non-replicating persistence (NRP). To understand the genetic basis of this growth restriction, a genetic selection was performed to identify mutants unable to arrest growth at acidic pH with propionate as a sole carbon source. The selection exclusively identified mutants in the PhoPR two-component regulatory system, which functions to modulate cell envelope lipids and redox homeostasis through the upregulation of lipid synthesis at acidic pH. Using genetic and chemical inhibition studies, we demonstrate that PhoPR arrests growth at acidic pH by diverting carbon away from the methyl citrate cycle towards lipid anabolism. Surprisingly, treatment of Mtb with pyrazinamide at acidic pH on propionate, also enabled growth. Therefore, this study defines new mechanisms by which Mtb integrates environmental signaling to regulate growth, metabolism, and drug susceptibility. These findings are relevant to pathogenesis, as PhoPR is essential for growth in macrophages and animals, environments with varying pH and carbon source availability, depending on immune pressures. These data suggest that drug susceptibility may be impacted by enhanced growth and metabolic capacity of Mtb in acidic and propionate-rich environments, such as the within the macrophage or the granuloma.

75 **Introduction**

76 *Mycobacterium tuberculosis* (Mtb) is a slow-growing pathogen that replicates within
77 macrophages or extracellularly. Depending on the conditions, the bacterium may be colonizing
78 environments with specific carbon sources and varying pH. The combinations of pH, carbon
79 source availability, and other environmental cues can impact Mtb growth rate and virulence.
80 During growth *in vitro*, or *in vivo*, Mtb has a slow doubling time of 20 hours to 70 days(1-3). Under
81 low oxygen, starvation, or mildly acidic pH on specific carbon sources, Mtb enters a non-
82 replicating persistent (NRP) state that allows the pathogen to arrest its growth while maintaining
83 its viability(4). Slow or arrested growth in mycobacteria is thought to play a role in establishing
84 tuberculosis-like diseases and can promote phenotypic drug tolerance and persistence(4-7).
85 Therefore, a mechanistic understanding of how Mtb regulates its growth rate, in response to
86 specific environmental cues, is necessary for understanding pathogenesis and characterizing
87 antibiotic susceptibility.

88 One of the key regulators of pH-driven adaptations in Mtb is the PhoPR two-component
89 regulatory system (TCS). PhoPR induces the expression of virulence-related genes in response
90 to acidic pH, magnesium, chloride and CO_2(8-11). These virulence-related genes include the
91 ESX-1 secretion system and cell envelope lipid synthesis genes such as *pks2*, *pks3* and *pks4*
92 which generate sulfolipid (SL) and other acylated trehalose lipids (12, 13). Notably, *phoPR*
93 mutants are highly attenuated in mice and guinea pigs (14, 15), making PhoPR a target for
94 vaccine development(16), supporting that PhoPR and adaptation to acidic pH or related cues are
95 critical for Mtb pathogenesis.

96 Our lab previously discovered that Mtb has restricted growth on specific single carbon
97 sources at acidic pH. Mtb grows well on carbon sources that function at the intersection of
98 glycolysis and the TCA cycle (e.g. pyruvate, acetate, oleic acid and cholesterol)(17). In contrast,
99 on other tested carbon sources, such as glycerol or propionate, Mtb fully arrests its growth at
100 acidic pH and establishes a state of NRP. We refer to this phenotype as acid growth arrest (17,

101 18). We hypothesized that Mtb has evolved means to restrict growth at acidic pH on specific
102 carbon sources to regulate growth and support pathogenesis. Indeed, we previously selected for
103 suppressor mutants of acid growth arrest in *ppe51* that enabled Mtb growth on glycerol at acidic
104 pH, increased its replication in infected activated macrophages, and resulted in decreased
105 fitness(18, 19). The goal of this study is to define the mechanisms of acid growth arrest on
106 propionate as a sole carbon source.

107 Significant research has been conducted examining propionyl-CoA metabolism in Mtb,
108 given it is a catabolic product of cholesterol, a carbon source consumed by Mtb in the host(20).
109 Propionyl-CoA is toxic to Mtb and is detoxified by the methyl citrate cycle (MCC) or by
110 incorporation into methyl branched lipids (such as phthiocerol dimycocerosates (PDIM), SL and
111 acylated trehaloses) (21, 22). The MCC is composed of the methyl-isocitrate lyases *icl1/icl2*
112 along with *prpC* and *prpD* (22). *icl1/icl2, prpC* and *prpD* are essential for growth in minimal media
113 supplemented with propionate (22-25). In the presence of vitamin B12, Mtb is able to survive in
114 the absence of the MCC, by promoting metabolism via methylmalonyl-CoA pathway, enabling the
115 sequestration of propionyl-CoA into methyl branched lipids such as PDIM (21, 22).

116 To define the mechanism of propionate-driven acid growth arrest, we conducted a forward
117 genetic selection for transposon (Tn) mutants that suppress acid growth arrest on propionate at
118 acidic pH. The selection exclusively identified Tn mutants in the PhoPR TCS. Based on these
119 findings, we propose a model where PhoPR arrests growth by diverting propionate towards the
120 synthesis of cell envelope lipids and, when mutated, growth is promoted by metabolism of
121 propionate by the MCC into pyruvate, a permissive carbon source for growth at acidic pH(17).
122 Additionally, we found that pyrazinamide (PZA) treatment also suppresses the acid growth arrest
123 phenotype in WT Mtb and on propionate PZA selectively sensitizes the *phoPR* mutant to killing
124 PZA. Together, these findings support a model linking acidic pH, carbon source, PhoPR signaling
125 and growth state for PZA activity.

126

127 **Results**

128 **PhoPR is required for acid growth arrest on propionate.**

129 We previously reported that Mtb grows on propionate at pH 7.0, but arrests growth on at
130 pH 5.7, based on changes in optical density (17). To determine if Mtb is viable and non-replicating,
131 we examined growth by optical density and CFUs over the course of 12 days of Mtb incubated on
132 propionate or pyruvate at pH 5.7. Mtb arrested growth on propionate (Figure 1A) and was viable
133 (Figure 1B), whereas pyruvate was permissive for growth. Therefore, like acid growth arrest on
134 glycerol, Mtb is non-replicating and viable during propionate-induced acid growth arrest.

135 We hypothesized that growth arrest on propionate is a regulated process and not intrinsic
136 to the carbon source itself, given that the carbon source can be metabolized at neutral pH and
137 Mtb is viable. To test this hypothesis, a forward genetic selection was performed to identify
138 suppressor mutants of acid growth arrest on propionate at acidic pH. An Mtb Erdman transposon
139 (Tn) mutant library containing ~100,000 mutants was plated on agar plates containing minimal
140 media buffered to pH 5.7 and supplemented with 2mM propionate as a sole carbon source.
141 Mutants with enhanced acidic growth (EAG) phenotype formed colonies on the plates following 8
142 weeks of incubation. In total, 20 colonies were isolated, and 16 were confirmed as mutants that
143 could grow on propionate (Figure 1C and Table S1). Using whole genome sequencing or inverse
144 PCR, we identified Tn insertion sites in 12 of the 16 confirmed mutants and all sequenced Tn
145 insertions were in *phoR or phoP,* including 6 independent insertions in *phoR and* one insertion in
146 *phoP.* (Supplemental Table 1). Notably, several of the isolated *phoR* mutants also had mutations
147 in the PDIM gene *ppsE*. We confirmed the phenotype of these mutants and observed the
148 *phoR*::Tn and *phoP*::Tn mutants grew on propionate at acidic pH, with higher growth in the
149 *phoR*::Tn mutant (Figure 1D). Using a *ΔphoPR* deletion mutant and complemented strain
150 previously generated in the CDC1551 background (10), we confirmed that at pH 5.7 on propionate
151 the *ΔphoPR* mutant demonstrated robust growth compared to the wildtype and the phenotype
152 was complemented (Figure 1E). There was no significant difference between strains at neutral

153 pH (Figure S1A). Therefore, we conclude that PhoPR is required for acidic growth arrest on
154 propionate at acidic pH.
155
156 **The *phoPR* mutant has enhanced growth on multiple carbon sources at acidic pH**
157 Previously, we established that *phoPR* is required to slow the growth of Mtb on the
158 permissive carbon source pyruvate at acidic pH(17). Therefore, we sought to determine if *phoPR*
159 is required for growth arrest on other carbon sources. We observed that the *ΔphoPR* mutant
160 displays enhanced growth on specific carbon sources that are permissive for growth at acidic pH
161 (pyruvate and acetate) and normally non-permissive for growth at acidic pH (propionate and
162 succinate), with the strongest enhanced growth phenotype observed in propionate (Figure 2).
163 We previously observed that acid growth arrest on glycerol was dependent on both pH
164 and carbon concentration(19). Therefore, we defined the interactions of pH and propionate
165 concentration on Mtb growth by testing growth at varying pH levels (pH 5.0-7.0), and propionate
166 concentrations (0 mM and 20 mM) (Figure 3 A-F). This assay was conducted in 96 well plates
167 where Mtb exhibits less robust growth, as compared to standing flask growth conditions used in
168 prior experiments. At 8 mM and 20 mM propionate, the *phoPR* mutant exhibited enhanced growth
169 at pHs 5.0-5.7, (Figure 3 A-C), whereas at pHs 6.0-7.0, the mutant had similar growth to the wild-
170 type. The Δ*phoPR* mutant exhibited a higher OD at 20 mM propionate, suggesting that growth is
171 proportionate to carbon source availability. Therefore, acid growth arrest is induced at pH 5.7 or
172 below. Notably, the PhoPR regulon is strongly induced pH below 6.0(9), consistent with the
173 induction of PhoPR signaling driving the growth arrest phenotype that we see. *pks2* is strongly
174 induced at acidic pH in a *phoPR*-dependent manner and is required for the synthesis of sulfolipids.
175 At acidic pH, we have previously shown that Mtb promotes SL synthesis and accumulation in a
176 *phoPR*-dependent manner(17). We previously isolated a *pks2::*Tn mutant and hypothesized that
177 if enhanced growth is a consequence of diversion of carbon from the TCA cycle, then the *pks2::Tn*
178 mutant should have enhanced growth on propionate. We examined the growth of the WT,

179 *phoR*::Tn and *pks2::Tn* mutants on propionate at acidic pH and observed that the *pks2::*Tn mutant
180 displayed an intermediate impact, with higher growth than the WT, but less than that of the *phoR*
181 mutant (Figure 1D). Therefore, the enhanced growth is also dependent on *pks2*, implicating
182 changes in lipid synthesis or the cell envelope composition in growth arrest.
183
184 **PhoPR is required for acidic pH-dependent cell death**
185 We were surprised to observe the *phoPR* mutant grow on propionate at pH 5.0 (Figure 3A).
186 This highly acidic pH can lead to cell death. Therefore, we examined WT, Δ*phoPR* mutant and
187 complemented strains for growth and viability over a 12-day time course in 2 mM propionate as
188 a sole carbon source, incubated in standing flasks. As anticipated, we observed a significant
189 reduction of WT OD and CFUs at acidic pH, indicating cell death, and an increase of CFUs for
190 the Δ*phoPR* mutant (Figure 4). Therefore, we conclude that cell death at acidic pH, is not an
191 intrinsic stress associated at acidic pH and instead dependent on PhoPR-dependent activities,
192 possibly related to remodeling of metabolism. Notably, the differences in growth between the pH
193 5.0 conditions in the dose response study (Figure 3A) and this experiment, are likely driven by
194 the more hypoxic conditions in the 96-well plates as compared to the standing flasks due to
195 differences in head space ratio, which is presumed to result in the more robust growth observed
196 in standing flasks.
197
198 **PhoPR restricts growth at acidic pH by diverting carbon from the methyl citrate cycle**
199 One of the key functions of PhoPR at acidic pH is envelope composition remodeling by
200 promoting lipid synthesis, including sulfolipids (SL), diacyltrehaloses (DAT) and
201 polyacyltrehaloses (PAT)(13). Deletion of *phoPR* results in a near complete loss of SL at acidic
202 pH, which is compensated for by the induction of triacylglycerol (TAG) (17). Propionyl-CoA is an
203 important substrate for the PhoPR-dependent synthesis of methyl-branched lipids such as SL,
204 DAT and PAT, as well as methyl-branched lipids synthesized independently of PhoPR, such as

205 PDIM and TAG. Given the partially enhanced growth of the *pks2* mutant (Figure 1D), we
206 hypothesized that growth arrest at acidic pH is due to PhoPR diverting carbon away from central
207 metabolism towards lipid metabolism, thus starving Mtb of carbon needed for growth. Indeed, a
208 similar phenomenon has been observed for hypoxia-driven growth arrest and the induction of *tgs1*
209 to produce TAG (26). We further hypothesize that in the PhoPR mutant, the propionate can be
210 metabolized into pyruvate via the methyl citrate cycle (MCC). Pyruvate is permissive for growth
211 at acidic pH, thus the redirection of propionate from lipid anabolism (in the WT) to pyruvate via
212 the MCC (in the *phoPR* mutant) could explain the enhanced growth of the Δ*phoPR* mutant on
213 propionate at acidic pH.

214 To first test this model, we examined if the MCC was required for growth on propionate at
215 acidic pH, using mutants in the methylisocitrate lyases *icl1/icl2* and complemented strains(24).
216 Lacking a *phoPR* mutant in the *icl1/icl2* mutant backgrounds, we used a chemical inhibitor of
217 *phoPR* signaling, ethoxzolamide (ETZ) (27), to downregulate PhoPR. The strains were cultured
218 in minimal media in propionate with or without ETZ, at acidic pH, and growth and viability were
219 monitored over 12 days(Figure 5A and S2A). In the DMSO control, the WT and *icl1* or *icl2* mutants
220 all had arrested growth at acidic pH, and the *icl1/icl2* exhibited a reduction of CFUs and OD, a
221 phenotype consistent with propionate toxicity in the absence of the MCC (Figure 5A and S2A). In
222 the ETZ-treated cells, we observed enhanced growth of the WT, consistent with PhoPR inhibition
223 driving growth at acidic pH (Figure 5A and S2A). The *icl1* and *icl2* mutants both had reduced
224 growth and viability (Figure 5A and S2A), with a the *icl2* mutant showing a greater reduction in
225 viability which could be driven by the direct regulation of Icl2 by propionate(28). Notably, at pH
226 7.0, the single *icl1* or *icl2* mutants grew well on propionate in both the DMSO and ETZ treated
227 cells, while the *icl1/icl2* mutant could not grow, due to propionate toxicity (Figure S3). To further
228 confirm the role of the MCC in *phoPR*-dependent enhanced growth, we examined if chemical
229 inhibition of Icl1/2 by itaconic acid (ITA) could inhibit the enhanced growth. Indeed, ITA completely

230 inhibited Mtb *phoPR* mutant growth on propionate at acidic pH (Figure S4). These data are
231 consistent with the MCC being required for enhanced growth of the Δ*phoPR* mutant at acidic pH.
232 To further validate the model that PhoPR-dependent diversion of carbon to lipid synthesis
233 promotes the growth arrest phenotype, we hypothesized that stimulating lipid synthesis in the
234 PhoPR mutant would suppress growth on propionate. To test this hypothesis, we examined
235 whether the induction of the methylmalonyl-CoA pathway, by the supplementation with vitamin
236 B12, reduces the growth of the PhoPR mutant. The WT, Δ*phoPR*, and complement strains were
237 grown in minimal media at acidic pH supplemented with propionate, with or without vitamin B12,
238 and growth and viability were monitored over 12 days. As hypothesized, vitamin B12 suppresses
239 the growth of the Δ*phoPR* mutant at acidic pH (Figure 5B and S2B), supporting that stimulating
240 lipid anabolism suppresses growth at acidic pH on propionate. Addition of vitamin B12 had no
241 impact on Mtb growth at pH 7.0 on propionate , in the WT or Δ*phoPR* mutant (Figure S2D),
242 supporting the phenotypes are acidic pH dependent.
243 Mtb increases the production of the TAG when *phoPR* is deleted, possibly as a
244 mechanism to balance redox homeostasis(17). We hypothesized that TAG synthesis may function
245 similarly as a sink for carbon and slow the growth of WT or the Δ*phoPR* mutant. To test this
246 hypothesis, we used a DosRST inhibitor, MSU-43996, that potently inhibits *tgs1* expression and
247 TAG synthesis (29). We examined the growth of WT, and the Δ*phoPR* mutant in the presence of
248 propionate, with or without 40 μM MSU-43996 at acidic pH and neutral pH (Figure 5C and S1B) .
249 When *tgs1* is inhibited, the WT exhibits enhanced growth, and the Δ*phoPR* mutant exhibits further
250 enhanced growth at acidic pH (Figure 5C and S2C); while no major differences are observed at
251 neutral pH (Figure S1B). These data further reinforce the hypothesis that lipid synthesis is slowing
252 or arresting Mtb growth at acidic pH.
253
254
255

256 **PhoPR restricts CoA at acidic pH**

257 We hypothesize that if PhoPR is diverting carbon away from central metabolism to slow growth,
258 this adaptation may be associated with less available CoA in the WT at acidic pH. In the Δ*phoPR*
259 mutant, metabolism of propionate into pyruvate would fuel the TCA cycle and promote increases
260 in CoA pools. To test this hypothesis, we examined total CoA in the WT, Δ*phoPR* mutant, and
261 complemented strains in 2mM propionate, 10 mM pyruvate or 10 mM glycerol at pH 5.7. During
262 growth arrest in propionate and glycerol, WT CoA pools remained relatively stable over the course
263 of six days (Figures 6A and S5). In contrast, on propionate CoA pools in the *phoPR* mutant
264 increased threefold at day 3 and then lowered again at day 6 (Figure 6A). There is no change
265 between day 0 and 6 in CoA in the growth arrested *phoPR* mutant in the presence of glycerol
266 (Figure S5). In pyruvate, which is growth permissive, CoA pools increased slightly in the WT and
267 were enhanced in the *phoPR* mutant, which also has enhanced growth in pyruvate (Figure 6C).
268 Consistent with our hypothesis, diversion of carbon from the TCA cycle to lipid synthesis by the
269 addition of vitamin B12, decreases the accumulation of CoA in the *phoPR* mutant (Figure 6B),
270 which is also associated with decreased growth (Figure 5B).

271 In our findings, total CoA in the *phoPR* mutant on propionate at acidic pH is negatively
272 associated with stimulation of lipid synthesis pathways and positively associated with growth. The
273 decrease in CoA pools at Day 6 in the *phoPR* mutant suggested that additional lipid synthesis
274 pathways may be engaged over time. The cultures are grown in standing flasks and we anticipate
275 that growth over 6 days by the *phoPR* mutant will consume oxygen and induce the *dosRST*
276 pathway. This would cause the strong induction of the TAG-synthase *tgs1* and provide an induced,
277 second mechanism to restrict growth under the hypoxic conditions caused by the growth of the
278 mutant. To test this hypothesis, we examined the impact of the *dosRST* inhibitor MSU-39446, on
279 CoA pools. In the MSU-39446 treated *phoPR* mutant the CoA pools did not decrease at day 6
280 (Figure 6D), a phenotype consistent with the enhanced growth caused by MSU-39446 treatment
281 (Figure 5C). Notably, CoA pools increased in the WT, a response consistent with the enhanced

282 growth of the WT (Figure 5C). Together, these data further support the hypothesis that growth
283 arrest on propionate at acidic pH is driven by restriction of central metabolism via synthesis of
284 PhoPR-dependent lipids.
285
286 **Pyrazinamide suppresses growth arrest on propionate at acidic pH.**
287 Pyrazinamide (PZA) activity is enhanced at acidic pH and its mechanism of action is
288 uncertain, but recent data suggests it may be associated with CoA metabolism and cell envelope
289 lipid homeostasis (17, 30-32). Therefore, we hypothesized that the WT strain and *phoPR* mutant
290 may exhibit differential sensitivity to PZA. To test this hypothesis, we examined the sensitivity of
291 WT, Δ*phoPR* mutant, and complemented strains to PZA across a dose range from 0-100 μM in
292 minimal medium supplemented with 2mM propionate at pH 5.7. Surprisingly, following 21 days of
293 incubation, PZA at concentrations of 2.5 and 10 μM suppressed acid growth arrest in the WT and
294 complemented strains (Figure 7A). However, the *phoPR* mutant was growth arrested under these
295 conditions, showing that it has enhanced sensitivity to PZA, as compared to the DMSO control,
296 where the *phoPR* mutant grew robustly. At a concentration of 1.25 μM, the growth of the WT and
297 *phoPR* mutant are about equal (Figure 7A) ,suggesting a complex interplay between PZA
298 concentration and modulation of growth at acidic pH on propionate.
299 The above assay was conducted in 96-well plates, and we sought to better characterize
300 the suppression of acid growth arrest by PZA in a standing flask-based acid growth arrest assay,
301 which exhibits more robust growth. WT, Δ*phoPR* mutant and complemented strains were
302 incubated at pH 5.7 with propionate as a sole carbon source, treated with 3.8 μM PZA, 20 μM
303 isoniazid (INH), or a DMSO control, and growth was monitored over 12 days. The WT and
304 complemented strains exhibited enhanced growth on PZA as compared to DMSO (Figure 7A and
305 7B), whereas the *phoPR* mutant was killed by PZA and showed robust growth in the DMSO control
306 (Figure 7D and 7E). We hypothesized that like enhanced growth of the Δ*phoPR* mutant, PZA may
307 also be causing enhanced growth by inhibiting lipid synthesis. To test this hypothesis, we

308 examined if additional of vitamin B12, limited the enhanced growth of PZA treated WT Mtb. As
309 hypothesized, vitamin B12 blocked the enhanced growth in the PZA treated Mtb (Figures S6 and
310 S7). INH inhibited the growth of all of the strains, showing the differential growth impact is PZA-
311 specific (Figure 7F and 7G). We also examined the impact of PZA sensitivity on the strains grown
312 on pyruvate and observed that that WT Mtb did not show enhanced growth on PZA, showing the
313 enhanced growth is propionate specific. (Figure S8). Notably, the Δ*phoPR* mutant was also more
314 sensitive to PZA on pyruvate (Figure S8) and INH on propionate (Fig. 7G), supporting that the
315 enhanced PZA sensitivity is not carbon source specific and the *phoPR* mutant is more sensitive
316 to distinct classes of antibiotics. To determine if the enhanced growth on WT Mtb on PZA is shared
317 between different strains, we also conducted this experiment in Mtb Erdman. We observed that
318 3.8 μM PZA caused enhanced growth of WT Erdman (Figure S9). No significant differences were
319 observed, between strains or treatments, when the experiment was replicated at neutral pH
320 (Figure S10), an expected result given the acidic pH-dependent activity of PZA. Together, these
321 findings show that PZA can result in enhanced growth or killing of Mtb depending on the pH,
322 concentration of PZA and PhoPR-signaling of the bacterium. This discovery generates further
323 complexity for understanding the mechanism of PZA function, as pH and carbon sources can vary
324 in different environments during infection, and differences in *phoPR* or *prpR* genotype and
325 function exist in clinical strains (33-35).
326
327 **Discussion**
328 Mtb remodels its physiology at acidic pH below ~6.5, demonstrating several pH-dependent
329 adaptations associated with pathogenesis and drug susceptibility(5, 36). Changes in carbon
330 metabolism are a substantial component of acidic pH-dependent adaptations. We and others
331 have observed that Mtb restricts its ability to grow on specific carbon sources at acidic pH, a
332 phenomenon we refer to as acid growth arrest. Previously, we found that Mtb arrests its growth
333 on glycerol and that this growth arrest is overcome by mutations *in ppe51* that promote enhanced

334 glycerol uptake (36). We concluded that growth arrest is overcome by increasing glycerol uptake
335 (36), possibly to overcome reduced glyceraldehyde-3-phosphate dehydrogenase activity at acidic
336 pH(37). *ppe51* mutants did not promote growth on other non-permissive carbon sources, including
337 propionate, leading us to hypothesize that acid growth arrest has different mechanisms for
338 different carbon sources.

339 The isolation of *phoPR* mutants that can grow on propionate strongly support our
340 hypothesis of carbon source specific metabolic restraints at acidic pH (Figure 8). For example,
341 *phoPR* mutants cannot grow on glycerol and *ppe51* EAG variants cannot grow on propionate.
342 Together, multiple independent observations support that the growth arrest on propionate is due
343 to the diversion of carbon towards the synthesis of PhoPR-dependent lipids (Figure 8). For
344 example, we observe growth arrest at acidic pH when methyl-branched lipid synthesis pathways
345 are activated on propionate, and when PhoPR-dependent pathways (SL, DAT and PAT), DosRST-
346 dependent pathways (TAG), or vitamin B12-dependent pathways (PDIM) are available to the
347 pathogen. Disruption of these pathways by deletion of *phoPR* (Fig. 8), interruption of the *phoPR*-
348 regulated gene *pks2* (Fig. 1*)*, inhibition of PhoPR-by treatment with ETZ (Fig. 5), inhibition of *tgs1*
349 expression by treatment with MSU-39446 (Fig. 8), or the absence of vitamin B12, results in the
350 enhanced acid growth phenotype. Notably, treatment with PZA also leads to enhanced acid
351 growth, suggesting part of PZA function may be related to inhibiting lipid synthesis. When lipid
352 synthesis is blocked, growth on propionate at acidic pH is dependent on the MCC, which is one
353 of primary mechanisms by which Mtb detoxifies propionate (38). Pyruvate is a permissive carbon
354 source at acidic pH, therefore, it is expected that if propionate is metabolized to pyruvate via the
355 MCC that it would promote growth (Figure 8). Given the many regulatory functions of PhoPR(39),
356 it remains possible that PhoPR is also regulating lipid-synthesis independent mechanisms to
357 arrest growth. Given the link between growth arrest and decreased CoA-pools, this could possibly
358 be a regulatory activity inhibiting central metabolism. We have also not explored the potential role

359 of cAMP signaling in the observed phenotypes, where PhoPR modulation of cAMP could be
360 impacting propionate detoxification mechanisms and cell envelope permeability(40, 41).
361 The presented data show that the PhoPR plays a role in the detoxification of propionate.
362 We observed that the DMSO treated WT strain and the single Δ*icl1* or Δ*icl2* mutants do not have
363 a survival defect (Figure. 5 and S2) and the double Δ*icl1/2* mutant has its viability reduced by ~1
364 log relatively to the starting CFUs. In contrast, when PhoPR signaling is inhibited by ETZ, viability
365 is reduced in Δ*icl2* mutants and in the Δ*icl1/2* double mutant by ~100 fold (Figure. 5 and S2). This
366 demonstrates that inhibition of PhoPR sensitizes Mtb to propionate toxicity. Therefore, PhoPR is
367 exerting dual functions under the tested conditions, to both arrest growth and detoxify propionate.
368 Mtb induces PhoPR at acidic pH on various carbon sources (glycerol, pyruvate,
369 propionate), and WT Mtb has a functional MCC, therefore, we do not believe that PhoPR is solely
370 induced specifically to detoxify propionate. Rather, we observed that the PhoPR mutant
371 experiences reductive stress at acidic pH, and we hypothesize that lipid synthesis serves the
372 purpose of oxidizing cofactors (such as NADPH to NADP+) to maintain redox homeostasis(17,
373 18). Consistent with this hypothesis, we observe that downregulation of SL production in the
374 *phoPR* mutant is associated with induction of other lipids such as TAG (17). Blocking both PhoPR
375 and DosRST pathways removes four of the major lipid synthesis pathways (SL, DAT, PAT and
376 TAG) and results in the most robust growth of propionate (Figure 5C, S2C). Pyruvate is known to
377 promote growth at acidic pH, and we hypothesize that by entering the TCA cycle near the
378 anaplerotic node provides Mtb the metabolic flexibility to maintain redox homeostasis by
379 balancing anabolism and catabolism, possibly via the PEP glyoxylate cycle(42, 43). In this
380 manner, if propionate is not diverted to lipid synthesis, it can be turned into a permissive carbon
381 source that balances redox homeostasis at the anaplerotic node, even in the absence of *phoPR*.
382 Similar to the mutations in *phoPR*, PZA at low concentrations can also suppress Mtb
383 growth arrest on propionate at acidic pH. Based on our model for propionate-dependent growth

384 arrest, we reason that PZA treatment may be acting to inhibit lipid synthesis, thus enabling more
385 propionate to be metabolized by the MCC into central metabolism. The mechanism of action of
386 PZA remains controversial, but recent evidence supports a role for CoA metabolism and changes
387 in cell envelope lipid synthesis playing a role in its activity (30, 44) . Resistance mutations to PZA
388 arise in PanD, which is involved in the synthesis of CoA. The PZA metabolite POA can bind to
389 PanD to inhibit CoA synthesis (32). Reduced CoA levels are predicted to result in lower levels of
390 lipid synthesis, as it is an essential cofactor in the initial steps of fatty acid activation. Notably, it
391 was recently reported that PDIM genes are strongly downregulated by treatment with PZA (45)
392 and PDIM mutants are associated with resistance to PZA (44). Therefore, we speculate enhanced
393 growth of the WT is due to reduced PDIM synthesis or other long-chain fatty acids that require
394 CoA for their synthesis. The small range of concentrations where this enhanced growth in the WT
395 is observed (~3 μM) may reflect a hypomorphic phenotype, where CoA metabolism is sufficiently
396 repressed by PZA to impact lipid metabolism, but not so much so to fully deplete CoA and kill the
397 cell. It is surprising that the Δ*phoPR* mutant is susceptible to PZA and does not have further
398 enhanced growth. Furthermore, the Δ*phoPR* mutant is more susceptible to PZA on both
399 propionate and pyruvate (Fig. 7 and Fig. S8), and INH on propionate (Fig. 7G), but rather
400 associated with enhanced growth at acidic pH. Because propionate is metabolized to pyruvate by
401 the MCC it is consistent with our model that PZA sensitivity would be similar on either propionate
402 and pyruvate. The Δ*phoPR* is also more sensitive to INH on propionate (Fig. 7G), suggesting
403 more general mechanisms be driving antibiotic susceptibility in the mutant. We speculate that an
404 alternative mechanism is driving PZA or INH sensitivity in the *phoPR* mutant, possibly differential
405 expression of a *phoPR* pathway independent on lipid anabolism. For example, a *ppe51* loss of
406 function mutant is reported to have enhanced susceptibility to PZA(46). *ppe51* is downregulated
407 in the *phoPR* mutant, suggesting it, or some other unknown PhoPR-regulated genes may play a
408 role in susceptibility that overcomes the expected further enhanced growth. Alternatively, the

409 *phoPR* mutant may have has increased permeability due to changes in the cell envelope or cAMP
410 signaling (13, 40, 47). It is possible that this increased permeability is increasing the intracellular
411 concentration of PZA or INH, accumulating to sufficient levels to inhibit growth.
412
413
414 **Concluding remarks**
415 The observation that PhoPR restricts growth on propionate at acidic pH is analogous to
416 the findings of Baek *et al*, who showed that the DosRST and hypoxia regulated gene *tgs1* inhibits
417 growth during hypoxia by diverting carbon from the TCA cycle(26). In both cases, growth
418 restriction is an environmental adaption and not an inherent metabolic limitation. TB disease is
419 caused by slow growing mycobacteria and persistence and growth arrest are associated with
420 drug tolerance. By understanding the complex mechanisms by which Mtb integrates
421 environmental cues, metabolism and growth arrest, we may define new drug targets that can
422 disrupt pathogenesis in a way the increases bacterial growth. Enhanced growth is associated with
423 reduced fitness in macrophages (36) and enhanced drug susceptibility *in vitro* (18). Therefore,
424 these non-traditional drug targets may have unique impacts during treatment, including treatment
425 shortening. Indeed, PZA was essential to shortening TB treatment times to six months and it is
426 tempting to speculate that some of this activity may be related to PZA enhancing Mtb growth in
427 mildly acidic and cholesterol rich environments, such as the macrophage or the granuloma. It is
428 also important to consider that *phoPR* and *prpR* have variants in clinical isolates (33-35),
429 supporting that the interplay of PhoPR and propionate observed in these studies, maybe
430 associated with differential pathogenesis and drug susceptibility and in human infections and drug
431 treatment.
432
433

434 **Methods**

435 **Bacterial strains and growth**

436 Mtb experiments were conducted with WT ERDMAN or WT CDC1551 as indicated. The Δ*phoPR*
437 deletion mutant, and complemented strains are in the CDC1551 background (10) and the *icl1/2*
438 mutants and complemented strains are in the Erdman background(24). Cultures were maintained
439 in 7H9 media supplemented with 10% OADC and .05% Tween-80. All single carbon source
440 experiments were performed in MMAT minimal media buffered to acidic pH 5.7 or pH 7.0(21),
441 using (1 g l−1 KH2PO4, 2.5 g l−1 Na2PO4, 0.5 g l−1 (NH4)2SO4, 0.15 g l−1 asparagine, 10 mg l−1
442 MgSO4, 50 mg l−1 ferric ammonium citrate, 0.1 mg l−1 ZnSO4, 0.5 mg l−1 CaCl2, and 0.05%
443 Tyloxapol) . For 12-day growth experiments, time points were taken every three days. For each
444 of our growth curve experiments, 2mM propionate was used unless stated otherwise. Chemical
445 inhibitors and supplements were used at the following concentrations: Ethoxzolamide at 40 μM,
446 MSU-39446 at 40 μM, Itaconic acid at 2 mM and vitamin B12 at 10ug/ml. Mtb was seeded in T-
447 25 standing tissue culture flasks in 8ml of minimal media at an initial cell density of 0.05 OD and
448 incubated at 37 °C and 5% CO_2. 500 μL of each culture was taken each day for optical density
449 measurements. Bacterial viability was assessed enumerating colony-forming units (CFUs) on
450 7H10+OADC plates.

451

452 **Genetic selection**

453 Transposon mutagenesis was performed in Mtb Erdman using the ϕMycoMarT7 Tn system as
454 previously described(48), generating a library with ~100,000 Tn mutants. The Tn mutant library
455 was plated on MMAT pH 5.7 agar plates supplemented with 2mM propionate as the sole carbon
456 source. Plates were incubated at 37°C, with mutants appearing around week 8 and isolated for
457 growth. Single-colony isolates were confirmed as EAG (enhanced acidic growth) mutants under
458 acidic conditions in liquid media MMAT pH 5.7 supplemented with 2mM propionate. The

459 transposon insertion sequences were confirmed using inverse PCR (49) or whole genome
460 sequencing.
461
462 **Whole Genome Sequencing**
463 Genomic DNA of selected mutants as well as the WT Erdman control was isolated, DNA libraries
464 were constructed, and sequenced using the Illumina MiSeqm in-paired end, 250 bp read format
465 (PE250). After the sequencing run, reads were demultiplexed and converted to FASTQ format
466 using the illumina bcl2 fastq (v1.8.4) script. The reads in the raw data files were then subjected
467 to trimming of low-quality bases and removal of adapter sequences using Trimmomatic v0.36,
468 with a 4 bp sliding window, and a read quality cutoff of below 15 or read length cutoff less than 36
469 bp. The trimmed reads were then aligned to the Erdman reference genome using the Burrow-
470 Wheeler alignments. Genome analysis tool kit base quality score recalibration, indel alignment,
471 and duplicate removal were applied, and SNP and INDEL discovery were performed.
472
473 **pH and propionate dose response combination growth assays**
474 Mtb cultures were incubated in a range of pH-buffered MMAT media ranging from pH 5.0-7.0 at a
475 starting OD of 0.2 in 96 well plates. Cultures were treated with a 2.5-fold serial dilution (0mM-
476 20mM) of propionate and incubated over a course of 21 days, with growth assessed by optical
477 density.
478
479 **Coenzyme A assay**
480 Coenzyme A was measured using a commercially available assay (Sigma-Aldrich). Cultures were
481 maintained in 7H9, and then seeded to an OD of 0.2 and resuspended in minimal media
482 supplemented with 2mM propionate in 8 ml of media. The assay measures both free CoA and
483 acyl-CoA. Total CoA was measured at Day 0, 3, and 6 and concentration determined using a
484 standard curve.

485

486 **Pyrazinamide Sensitivity Assays**

487 Dose response assays were conducted in a 96 well plate cultures seeded at OD 0.2 and in
488 minimal media supplemented with 2mM propionate across a dose response from 100 μM-0 μM
489 of PZA. Plates were incubated for 6 days in a sealed Ziploc bag at 37C and OD read on a plate
490 reader. Standing flask assays were conducted using conditions as described earlier in the
491 methods. WTCDC, Δ*phoPR* mutant, and complement were grown in minimal media at acidic pH
492 supplemented with propionate and treated with DMSO, 3.84 uM Pyrazinamide, and 20uM
493 Isoniazid using conditions described above. Growth was measured Day 0, 3, 6, 9, and 12.
494 Viability was measured Day 0 and Day 12 by enumerating CFUs.

495

496 **Acknowledgements**

497 We thank Prof. John McKinney for sharing the *icl1/icl2* mutant strains. Research on this project
498 was supported by grants from the NIAID (R01 AI116605 and R01 AI150855) and AgBioResearch.

499

500 **Figure Legends**

501 **Figure 1. PhoPR arrests growth on propionate at acidic pH**. A) Growth curves of WT Mtb CDC
502 strain grown in acidic pH for 12 days, in media supplemented with propionate or pyruvate. B)
503 Bacterial viability evaluated using CFUs plated at days 0 and 12, demonstrating the viability of
504 the growth-arrested bacteria under propionate. C) Relative growth of 16 different transposon
505 mutants with enhanced growth on propionate relative to the WT (dotted line). All sequenced
506 mutants were in *phoR or phoP* (Supplemental Table 1). D) Growth curves of transposon mutants
507 in *phoR*, *phoP* and *pks2*, grown at acidic pH in minimal media supplemented with 2mM
508 propionate. E) Growth curves of Δ*phoPR* mutant and complemented strain compared to WT CDC
509 strain showing growth of the *phoPR* mutant. Multiple comparison unpaired t-test was used for the

510 growth curves analysis while one-way ANOVA was used for the viability analysis, * <0.05, **
511 <0.01, *** <0.001, **** <0.0001. Experiments were replicated at least twice with similar results.
512
513 **Figure 2. The ΔPhoPR has enhanced growth on specific carbon sources at acidic pH.** Mtb
514 growth was evaluated on various carbon sources after 21 days incubation. The Δ*phoPR* mutant
515 exhibits enhanced growth at acidic pH on selected permissive (acetate and pyruvate) and non-
516 permissive carbon sources (propionate and succinate). Two-way ANOVA was used for statistical
517 analysis, * <0.05, ** <0.01, *** <0.001, **** <0.0001. Experiments were replicated at least twice
518 with similar results.
519
520 **Figure 3. Enhanced growth of the Δ*phoPR* mutant is dependent on level of pH and**
521 **propionate concentration.** Growth of the Δ*phoPR* mutant, the WT and complemented strains
522 was tested in minimal media supplemented with a range of concentrations of propionate (20 mM
523 to 0.16 mM) at different pHs (5.0-7-.0). The Δ*phoPR* mutant has enhanced growth in dependent
524 on propionate concentration at pHs of 5.0, 5.5 and 5.7 (**A-C**), but not 6-7 (**D-F**). A multiple
525 comparison unpaired t-test was used for this analysis, * <0.05, ** <0.01, *** <0.001, **** <0.0001.
526 Experiments were replicated at least twice with similar results.
527
528 **Figure 4. PhoPR is required for cell death at pH 5.0. A)** The WT, Δ*phoPR* mutant, and
529 complemented strain were incubated at acidic pH for 12 days, in minimal media supplemented
530 with propionate. The Δ*phoPR* mutant has enhanced growth compared to the WT, a phenotype
531 that is complemented. **B)** Viability assays, show that the WT and complemented strains exhibit
532 cell death at pH 5.0, while the *phoPR* mutant grows. A multiple comparison unpaired t-test was
533 used for this analysis, * <0.05, ** <0.01, *** <0.001, **** <0.0001. Experiments were replicated at
534 least twice with similar results.

535

536 **Figure 5. PhoPR restricts growth at acidic pH by diverting carbon from the methyl citrate**
537 **cycle. A)** Growth curves of the WT, knockout strain of isocitrate lyases 1 and/or 2, and the
538 complemented strains, treated with DMSO or ethoxzolamide (ETZ), an indirect inhibitor of PhoPR,
539 showing a significant reduction in growth in the *icl2* and double knockout strains. **B)** Growth
540 curves conducted in wildtype, *phoPR* mutant, and complemented strains in minimal media
541 buffered to pH 5.7 supplemented with 2mM propionate and vitamin B12 over a course of 12 days,
542 showing vitamin B12 suppresses enhanced growth in the Δ*phoPR* mutant strain.**C)** Growth of the
543 WT, Δ*phoPR* mutant, and complement strains treated with MSU-43996 or the DMSO control,
544 showing an enhanced growth in the presence of MSU-43996 treatment. An unpaired t-test was
545 used between individual groups and the WT for the growth curves, while a one-way ANOVA was
546 used for the viability experiments, * <0.05, ** <0.01, *** <0.001, **** <0.0001. Experiments were
547 replicated at least twice with similar results.

548

549 **Figure 6: Enhanced acid growth is associated with increased CoA pools. A)** CoA pools in
550 the Δ*phoPR* mutant, WT CDC, and complemented strain grown in minimal media supplemented
551 with 2 mM propionate at acidic pH, showing enhanced metabolic capacity (i.e., higher CoA pools)
552 in the Δ*phoPR* mutant during the first three days of growth ($p = 0.006$), which significantly
553 decreases around day 6 ($p = 0.009$). **B)** CoA pools in the three strains, grown in minimal media
554 supplemented with vitamin B12 at acidic pH, showing no significant differences between the three
555 strains throughout the 6-day growth period. **C)** CoA pools in the three strains, grown in minimal
556 media supplemented with 10 mM of pyruvate at acidic pH, showing enhanced metabolic capacity
557 of the Δ*phoPR* mutant and WT through day 6. **D)** CoA pools in the three strains, grown in minimal
558 media supplemented with 40 μM of MSU-43996 at acidic pH, showing enhanced metabolic
559 capacity of the Δ*phoPR* mutant when *tgs1*, a is inhibited. Two-way ANOVA was used for this

560 analysis, * <0.05, ** <0.01, *** <0.001, **** <0.0001. Experiments were replicated at least twice
561 with similar results.
562
563 **Figure 7: PZA suppresses acid growth arrest on propionate. A)** Dose-response relationship
564 of pyrazinamide (100-0 μM) in the Δ*phoPR* null mutant, WT, and complement strains, conducted
565 in minimal media supplemented with 2mM propionate at acidic pH, demonstrating enhanced
566 growth of the WT and complemented strains on PZA at concentrations between 5.0-2.5 μM. **B**
567 **and C)** Assessment of the growth (B) and viability (C) of the three strains in minimal media
568 supplemented with 2mM propionate at acidic pH, treated with the vehicle as a control, showing
569 enhanced growth of the Δ*phoPR* mutant. **D and E)** Assessment of the growth (D) and viability (E)
570 of the three strains in minimal media supplemented with 2mM propionate at acidic pH treated with
571 PZA (3.84 μM), demonstrating enhanced growth of the WT and higher sensitivity of the Δ*phoPR*
572 mutant. **F and G)** Assessment of the growth (F) and viability (G) of the three strains in minimal
573 media supplemented with 2mM propionate at acidic pH treated with isoniazid (INH, 20 μM),
574 demonstrating similar levels of sensitivity in the three strains. Multiple comparison T-test was used
575 for the growth curves analysis, while Two-way ANOVA was used for the viability, * <0.05, ** <0.01,
576 *** <0.001, **** <0.0001. Experiments were replicated at least twice with similar results.
577
578 **Figure 8: Model for Mtb growth arrest on propionate at acidic pH and mechanisms of**
579 **suppression by mutations in *phoPR* or pyrazinamide treatment.** Propionate-dependent acid
580 growth arrest is a PhoPR-regulated response driven by diversion of carbon away from central
581 metabolism and into the synthesis lipids. At acidic pH, propionyl-CoA is used as a substrate to
582 synthesize methyl-branched lipids, either through the polyketide synthases Pks2, Pks3 and Pks4,
583 or through the methyl-malonyl pathway. Additionally, the enzyme MutAB, a vitamin B12-
584 dependent enzyme, catalyzes the reversible interconversion between malonyl-CoA and succinyl-

585 CoA, contributing to the synthesis of branched lipids. In either cases, low pH triggers remodeling
586 of central metabolism towards complex lipids synthesis to alter the mycomembrane structure as
587 a pH-dependent adaptation, consuming the CoA pools and slowing, or arresting growth in the
588 process. This pH-dependent adaptation in lost in the *phoPR* null mutant or under indirect PhoPR
589 chemical inhibition using ethoxzolamide (ETZ). Instead, the propionate is metabolized into
590 pyruvate by the methylcitrate cycle, a permissive carbon source, increasing CoA pools and
591 permitting fast growth. Additionally, at acidic pH, the *phoPR* null mutant upregulates triacylglycerol
592 synthesis using tgs1. Chemical inhibition of *tgs1* using MSU-39446 prevents diversion of CoA
593 pools into TAG synthesis and away from central metabolism, increasing CoA pools, metabolism
594 and growth in both the WT and *phoPR* null mutant. PZA treatment causes enhanced growth in
595 the WT, which may be driven by inhibiting lipid synthesis via depletion of CoA pools.
596
597
598
599
600
601
602
603
604
605
606
607

608 **References**

609

610 1. Gill WP, Harik NS, Whiddon MR, Liao RP, Mittler JE, Sherman DR. 2009. A replication
611 clock for Mycobacterium tuberculosis. Nat Med 15:211-4.

612 2. Rohde KH, Veiga DF, Caldwell S, Balazsi G, Russell DG. 2012. Linking the transcriptional
613 profiles and the physiological states of Mycobacterium tuberculosis during an extended
614 intracellular infection. PLoS Pathog 8:e1002769.

615 3. Munoz-Elias EJ, Timm J, Botha T, Chan WT, Gomez JE, McKinney JD. 2005. Replication
616 dynamics of Mycobacterium tuberculosis in chronically infected mice. Infect Immun
617 73:546-51.

618 4. Zheng H, Abramovitch RB. 2019. Host-pathogen interactions influencing Mycobacterium
619 tuberculosis persistence and drug tolerance *In* Lewis K (ed), Persister Cells and Infectious
620 Disease. Springer.

621 5. Baker JJ, Dechow SJ, Abramovitch RB. 2019. Acid Fasting: Modulation of Mycobacterium
622 tuberculosis Metabolism at Acidic pH. Trends Microbiol 27:942-953.

623 6. Adams KN, Takaki K, Connolly LE, Wiedenhoft H, Winglee K, Humbert O, Edelstein PH,
624 Cosma CL, Ramakrishnan L. 2011. Drug tolerance in replicating mycobacteria mediated
625 by a macrophage-induced efflux mechanism. Cell 145:39-53.

626 7. Liu Y, Tan S, Huang L, Abramovitch RB, Rohde KH, Zimmerman MD, Chen C, Dartois V,
627 VanderVen BC, Russell DG. 2016. Immune activation of the host cell induces drug
628 tolerance in Mycobacterium tuberculosis both in vitro and in vivo. J Exp Med 213:809-25.

629 8. Walters SB, Dubnau E, Kolesnikova I, Laval F, Daffe M, Smith I. 2006. The *Mycobacterium*
630 *tuberculosis* PhoPR two-component system regulates genes essential for virulence and
631 complex lipid biosynthesis. Molecular Microbiology 60:312-330.

632 9. Abramovitch RB, Rohde KH, Hsu FF, Russell DG. 2011. *aprABC*: a *Mycobacterium*
633 *tuberculosis* complex-specific locus that modulates pH-driven adaptation to the
634 macrophage phagosome. Mol Microbiol 80:678-94.

635 10. Tan S, Sukumar N, Abramovitch RB, Parish T, Russell DG. 2013. Mycobacterium
636 tuberculosis Responds to Chloride and pH as Synergistic Cues to the Immune Status of
637 its Host Cell. PLoS Pathog 9:e1003282.

638 11. Dechow SJ, Goyal R, Johnson BK, Haiderer ER, Abramovitch RB. 2025. Carbon dioxide
639 regulates Mycobacterium tuberculosis PhoPR signaling and virulence. Infect Immun
640 93:e0056824.

641 12. Feng L, Chen S, Hu Y. 2018. PhoPR Positively Regulates whiB3 Expression in Response
642 to Low pH in Pathogenic Mycobacteria. J Bacteriol 200.

643 13. Asensio JG, Maia C, Ferrer NL, Barilone N, Laval F, Soto CY, Winter N, Daffe M, Gicquel
644 B, Martin C, Jackson M. 2006. The virulence-associated two component PhoP-PhoR

645 system controls the biosynthesis of polyketide-derived lipids in *Mycobacterium*
646 *tuberculosis*. Journal of Biological Chemistry 281:1313-1316.

647 14. Perez E, Samper S, Bordas Y, Guilhot C, Gicquel B, Martin C. 2001. An essential role for
648 *phoP* in *Mycobacterium tuberculosis* virulence. Molecular Microbiology 41:179-187.

649 15. Martin C, Williams A, Hernandez-Pando R, Cardona PJ, Gormley E, Bordat Y, Soto CY,
650 Clark SO, Hatch GJ, Aguilar D, Ausina V, Gicquel B. 2006. The live *Mycobacterium*
651 *tuberculosis phoP* mutant strain is more attenuated than BCG and confers protective
652 immunity against tuberculosis in mice and guinea pigs. Vaccine 24:3408-3419.

653 16. Luabeya AKK, Rozot V, Imbratta C, Ratangee F, Shenje J, Tameris M, Mendelsohn SC,
654 Geldenhuys H, Fisher M, Musvosvi M, Young C, Mulenga H, Bilek N, Mabwe S, Jelsbak
655 IM, Rodriguez E, Puentes E, Doce J, Aguilo N, Martin C, Pillay C, Tait D, Russell M, Van
656 Der Merve A, Rutkowski K, Hunt D, Ginsberg A, Scriba TJ, Hatherill M, team A. 2025. Live-
657 attenuated Mycobacterium tuberculosis vaccine, MTBVAC, in adults with or without M
658 tuberculosis sensitisation: a single-centre, phase 1b-2a, double-blind, dose-escalation,
659 randomised controlled trial. Lancet Glob Health 13:e1030-e1042.

660 17. Baker JJ, Johnson BK, Abramovitch RB. 2014. Slow growth of Mycobacterium
661 tuberculosis at acidic pH is regulated by phoPR and host-associated carbon sources. Mol
662 Microbiol 94:56-69.

663 18. Baker JJ, Abramovitch RB. 2018. Genetic and metabolic regulation of Mycobacterium
664 tuberculosis acid growth arrest. Sci Rep 8:4168.

665 19. Dechow SJ, Baker JJ, Murto M, Abramovitch RB. 2022. ppe51 Variants Enable Growth of
666 Mycobacterium tuberculosis at Acidic pH by Selectively Promoting Glycerol Uptake. J
667 Bacteriol 204:e0021222.

668 20. VanderVen BC, Fahey RJ, Lee W, Liu Y, Abramovitch RB, Memmott C, Crowe AM, Eltis
669 LD, Perola E, Deininger DD, Wang T, Locher CP, Russell DG. 2015. Novel inhibitors of
670 cholesterol degradation in Mycobacterium tuberculosis reveal how the bacterium's
671 metabolism is constrained by the intracellular environment. PLoS Pathog 11:e1004679.

672 21. Lee W, VanderVen BC, Fahey RJ, Russell DG. 2013. Intracellular Mycobacterium
673 tuberculosis exploits host-derived fatty acids to limit metabolic stress. J Biol Chem
674 288:6788-800.

675 22. Savvi S, Warner DF, Kana BD, McKinney JD, Mizrahi V, Dawes SS. 2008. Functional
676 characterization of a vitamin B-12-dependent methylmalonyl pathway in *Mycobacterium*
677 *tuberculosis*: Implications for propionate metabolism during growth on fatty acids. Journal
678 of Bacteriology 190:3886-3895.

679 23. Gould TA, van de Langemheen H, Munoz-Elias EJ, McKinney JD, Sacchettini JC. 2006.
680 Dual role of isocitrate lyase 1 in the glyoxylate and methylcitrate cycles in Mycobacterium
681 tuberculosis. Mol Microbiol 61:940-7.

682 24. Munoz-Elias EJ, McKinney JD. 2005. Mycobacterium tuberculosis isocitrate lyases 1 and
683 2 are jointly required for in vivo growth and virulence. Nat Med 11:638-44.

684 25. Upton AM, McKinney JD. 2007. Role of the methylcitrate cycle in propionate metabolism
685 and detoxification in Mycobacterium smegmatis. Microbiology 153:3973-82.

686 26. Baek SH, Li AH, Sassetti CM. 2011. Metabolic regulation of mycobacterial growth and
687 antibiotic sensitivity. PLoS Biol 9:e1001065.

688 27. Johnson BK, Colvin CJ, Needle DB, Mba Medie F, Champion PA, Abramovitch RB. 2015.
689 The Carbonic Anhydrase Inhibitor Ethoxzolamide Inhibits the Mycobacterium tuberculosis
690 PhoPR Regulon and Esx-1 Secretion and Attenuates Virulence. Antimicrob Agents
691 Chemother 59:4436-45.

692 28. Bhusal RP, Jiao W, Kwai BXC, Reynisson J, Collins AJ, Sperry J, Bashiri G, Leung IKH.
693 2019. Acetyl-CoA-mediated activation of Mycobacterium tuberculosis isocitrate lyase 2.
694 Nat Commun 10:4639.

695 29. Zheng H, Williams JT, Aleiwi B, Ellsworth E, Abramovitch RB. 2020. Inhibiting
696 Mycobacterium tuberculosis DosRST Signaling by Targeting Response Regulator DNA
697 Binding and Sensor Kinase Heme. ACS Chem Biol 15:52-62.

698 30. Thiede JM, Dillon NA, Howe MD, Aflakpui R, Modlin SJ, Hoffner SE, Valafar F, Minato Y,
699 Baughn AD. 2021. Pyrazinamide Susceptibility Is Driven by Activation of the SigE-
700 Dependent Cell Envelope Stress Response in Mycobacterium tuberculosis. mBio
701 13:e0043921.

702 31. Gopal P, Gruber G, Dartois V, Dick T. 2019. Pharmacological and Molecular Mechanisms
703 Behind the Sterilizing Activity of Pyrazinamide. Trends Pharmacol Sci 40:930-940.

704 32. Gopal P, Yee M, Sarathy J, Low JL, Sarathy JP, Kaya F, Dartois V, Gengenbacher M, Dick
705 T. 2016. Pyrazinamide Resistance Is Caused by Two Distinct Mechanisms: Prevention of
706 Coenzyme A Depletion and Loss of Virulence Factor Synthesis. ACS Infect Dis 2:616-626.

707 33. Liu Q, Zhu J, Dulberger CL, Stanley S, Wilson S, Chung ES, Wang X, Culviner P, Liu YJ,
708 Hicks ND, Babunovic GH, Giffen SR, Aldridge BB, Garner EC, Rubin EJ, Chao MC,
709 Fortune SM. 2022. Tuberculosis treatment failure associated with evolution of antibiotic
710 resilience. Science 378:1111-1118.

711 34. Malaga W, Payros D, Meunier E, Frigui W, Sayes F, Pawlik A, Orgeur M, Berrone C,
712 Moreau F, Mazeres S, Gonzalo-Asensio J, Rengel D, Martin C, Astarie-Dequeker C,
713 Mourey L, Brosch R, Guilhot C. 2023. Natural mutations in the sensor kinase of the PhoPR
714 two-component regulatory system modulate virulence of ancestor-like tuberculosis bacilli.
715 PLoS Pathog 19:e1011437.

716 35. Hicks ND, Yang J, Zhang X, Zhao B, Grad YH, Liu L, Ou X, Chang Z, Xia H, Zhou Y, Wang
717 S, Dong J, Sun L, Zhu Y, Zhao Y, Jin Q, Fortune SM. 2018. Clinically prevalent mutations
718 in Mycobacterium tuberculosis alter propionate metabolism and mediate multidrug
719 tolerance. Nat Microbiol 3:1032-1042.

720 36. Dechow SJ, Abramovitch RB. 2024. Targeting Mycobacterium tuberculosis pH-driven
721 adaptation. Microbiology (Reading) 170.

722 37. Gouzy A, Healy C, Black KA, Rhee KY, Ehrt S. 2021. Growth of Mycobacterium
723 tuberculosis at acidic pH depends on lipid assimilation and is accompanied by reduced
724 GAPDH activity. Proc Natl Acad Sci U S A 118.

725 38. Savvi S, Warner DF, Kana BD, McKinney JD, Mizrahi V, Dawes SS. 2008. Functional
726 characterization of a vitamin B12-dependent methylmalonyl pathway in Mycobacterium
727 tuberculosis: implications for propionate metabolism during growth on fatty acids. J
728 Bacteriol 190:3886-95.

729 39. Broset E, Martin C, Gonzalo-Asensio J. 2015. Evolutionary landscape of the
730 Mycobacterium tuberculosis complex from the viewpoint of PhoPR: implications for
731 virulence regulation and application to vaccine development. MBio 6:e01289-15.

732 40. Khan H, Paul P, Goar H, Bamniya B, Baid N, Sarkar D. 2024. Mycobacterium tuberculosis
733 PhoP integrates stress response to intracellular survival by regulating cAMP level. Elife
734 13.

735 41. McDowell JR, Bai G, Lasek-Nesselquist E, Eisele LE, Wu Y, Hurteau G, Johnson R, Bai
736 Y, Chen Y, Chan J, McDonough KA. 2023. Mycobacterial phosphodiesterase Rv0805 is a
737 virulence determinant and its cyclic nucleotide hydrolytic activity is required for propionate
738 detoxification. Mol Microbiol 119:401-422.

739 42. Munoz-Elias EJ, McKinney JD. 2006. Carbon metabolism of intracellular bacteria. Cell
740 Microbiol 8:10-22.

741 43. Sauer U, Eikmanns BJ. 2005. The PEP-pyruvate-oxaloacetate node as the switch point
742 for carbon flux distribution in bacteria. FEMS Microbiol Rev 29:765-94.

743 44. Gopal P, Sarathy JP, Yee M, Ragunathan P, Shin J, Bhushan S, Zhu J, Akopian T, Kandror
744 O, Lim TK, Gengenbacher M, Lin Q, Rubin EJ, Gruber G, Dick T. 2020. Pyrazinamide
745 triggers degradation of its target aspartate decarboxylase. Nat Commun 11:1661.

746 45. Ostrer L, Crooks TA, Howe MD, Vo S, Jia Z, Hegde P, Schacht N, Aldrich CC, Baughn AD.
747 2025. Mechanism of the Dual Action Self-Potentiating Antitubercular Drug
748 Morphazinamide. bioRxiv doi:10.1101/2024.10.08.617272.

749 46. Bellerose MM, Baek SH, Huang CC, Moss CE, Koh E, Proulx M, Smith C, Baker RE, Lee
750 JS, Eum S, Shin SJ, Cho SN, Murray M, Sassetti CM. 2019. Common variants in the
751 glycerol kinase gene reduce tuberculosis drug efficacy. mBio in press.

752 47. Jackson M, Raynaud C, Laneelle MA, Guilhot C, Laurent-Winter C, Ensergueix D, Gicquel
753 B, Daffe M. 1999. Inactivation of the antigen 85C gene profoundly affects the mycolate
754 content and alters the permeability of the Mycobacterium tuberculosis cell envelope. Mol
755 Microbiol 31:1573-87.

756 48. Long JE, DeJesus M, Ward D, Baker RE, Ioerger T, Sassetti CM. 2015. Identifying
757 essential genes in Mycobacterium tuberculosis by global phenotypic profiling. Methods
758 Mol Biol 1279:79-95.

759 49. Ochman H, Gerber AS, Hartl DL. 1988. Genetic applications of an inverse polymerase
760 chain reaction. Genetics 120:621-3.

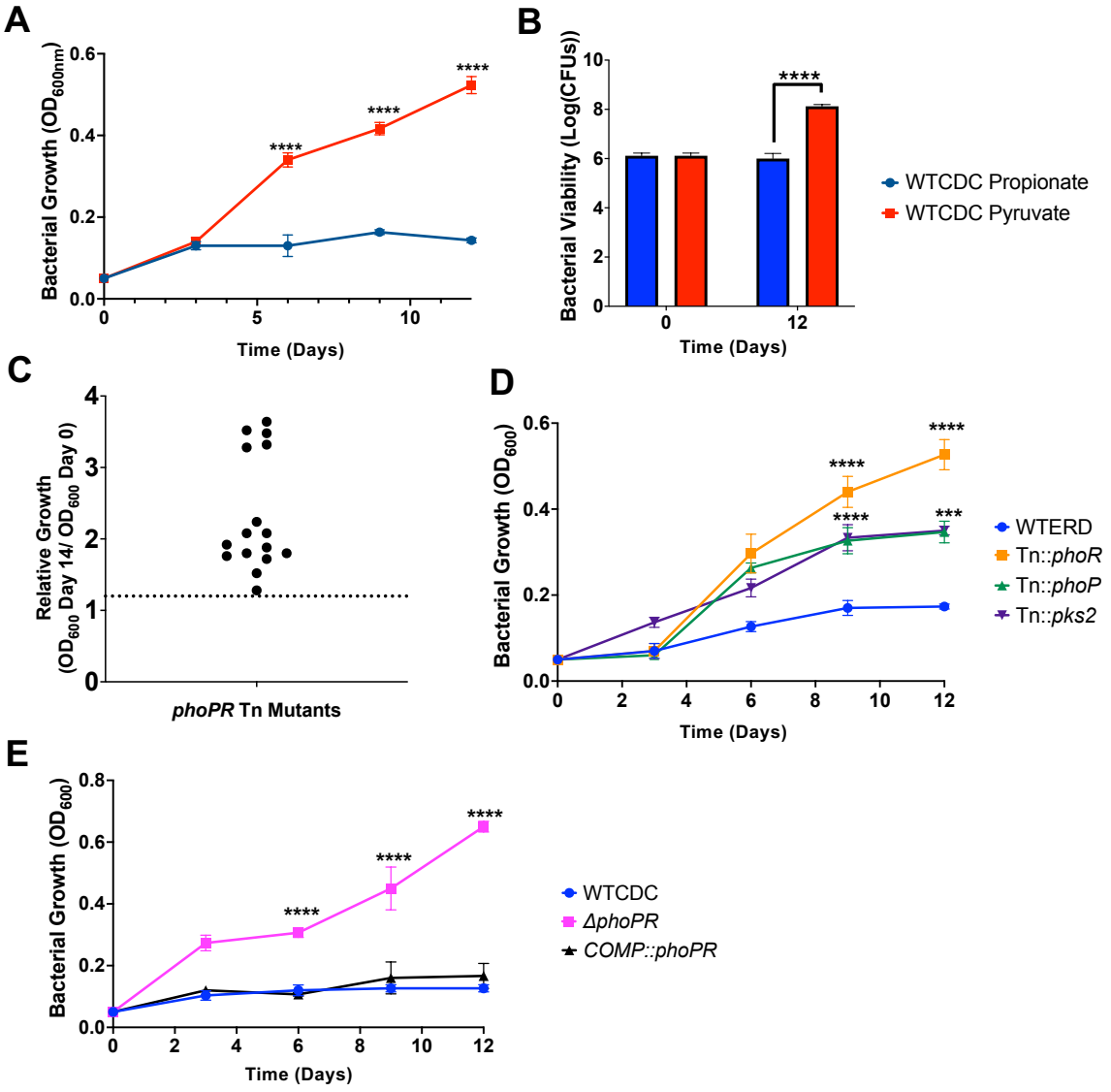
A
Bacterial Growth (OD_{600nm})
0.0
0.2
0.4
0.6
0
5
10
Time (Days)
****
****
****
B
Bacterial Viability (Log(CFUs))
0
2
4
6
8
10
0
12
Time (Days)
****
WTCDC Propionate
WTCDC Pyruvate
C
Relative Growth
(OD_{600} Day 14/ OD_{600} Day 0)
0
1
2
3
4
phoPR Tn Mutants
D
Bacterial Growth (OD_{600})
0.0
0.2
0.4
0.6
0
2
4
6
8
10
12
Time (Days)
****
****
****
***
WTERD
Tn::*phoR*
Tn::*phoP*
Tn::*pks2*
E
Bacterial Growth (OD_{600})
0.0
0.2
0.4
0.6
0.8
0
2
4
6
8
10
12
Time (Days)
****
****
****
WTCDC
ΔphoPR
COMP::phoPR

Figure 1

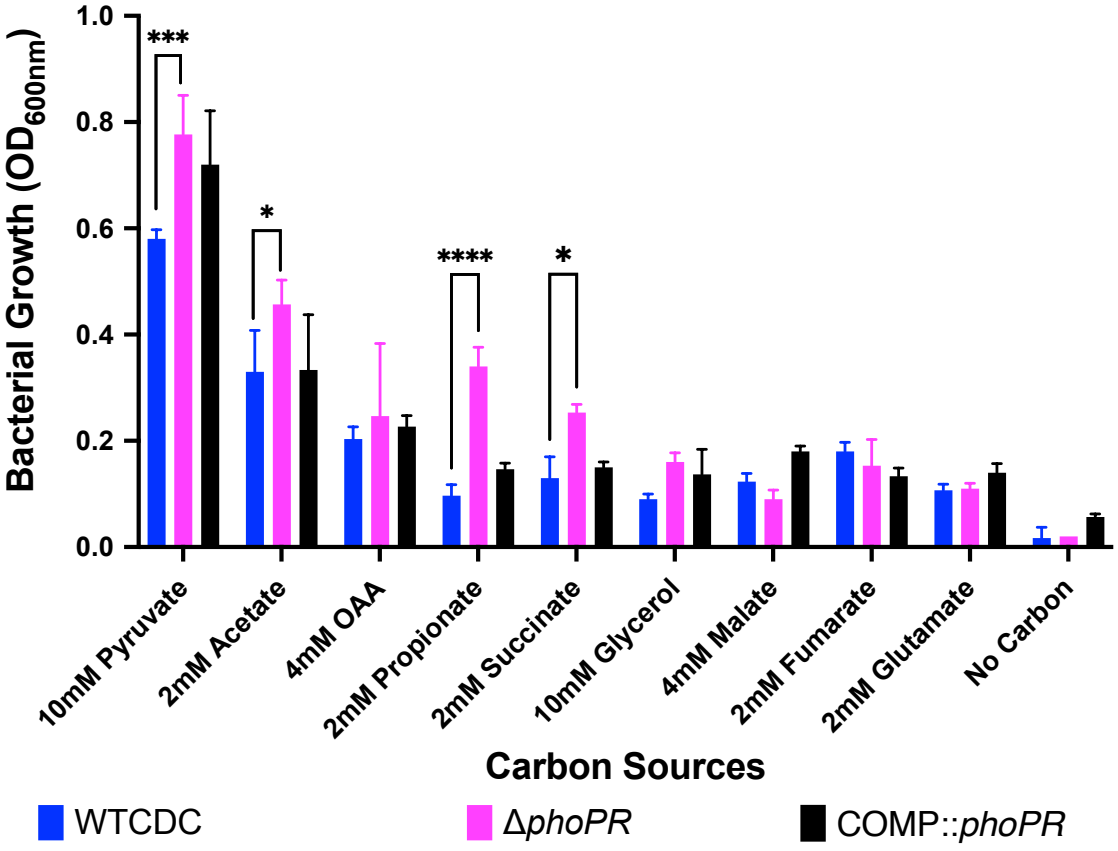
Bacterial Growth (OD600nm)
1.0
0.8
0.6
0.4
0.2
0.0
***
*
****
*
10mM Pyruvate
2mM Acetate
4mM OAA
2mM Propionate
2mM Succinate
10mM Glycerol
4mM Malate
2mM Fumarate
2mM Glutamate
No Carbon
Carbon Sources
WTCDC
ΔphoPR
COMP::phoPR

Figure 2

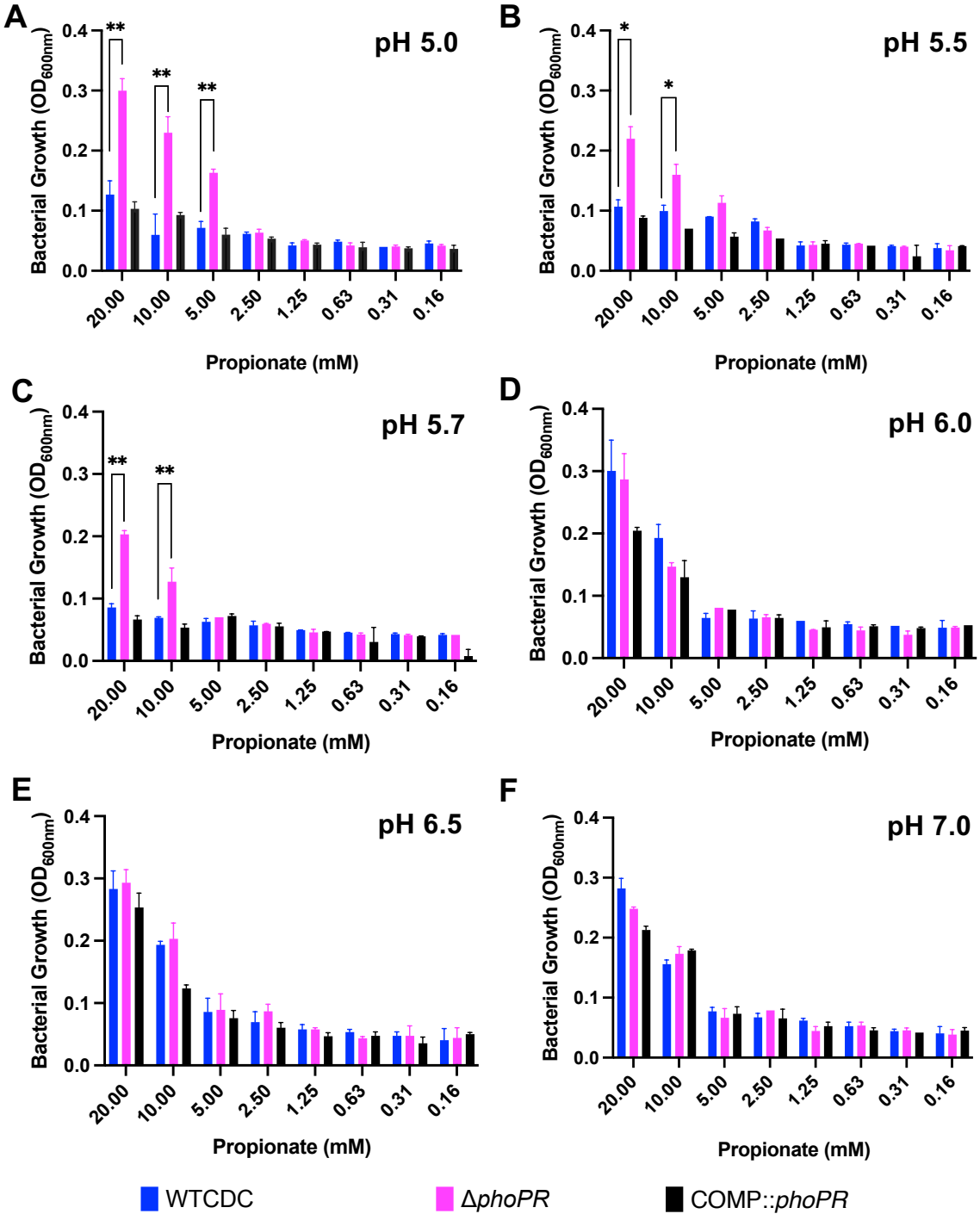
A
pH 5.0
B
pH 5.5
C
pH 5.7
D
pH 6.0
E
pH 6.5
F
pH 7.0
Bacterial Growth (OD600nm)
Propionate (mM)
20.00
10.00
5.00
2.50
1.25
0.63
0.31
0.16
0.0
0.1
0.2
0.3
0.4
*
**
WTCDC
ΔphoPR
COMP::phoPR

Figure 3

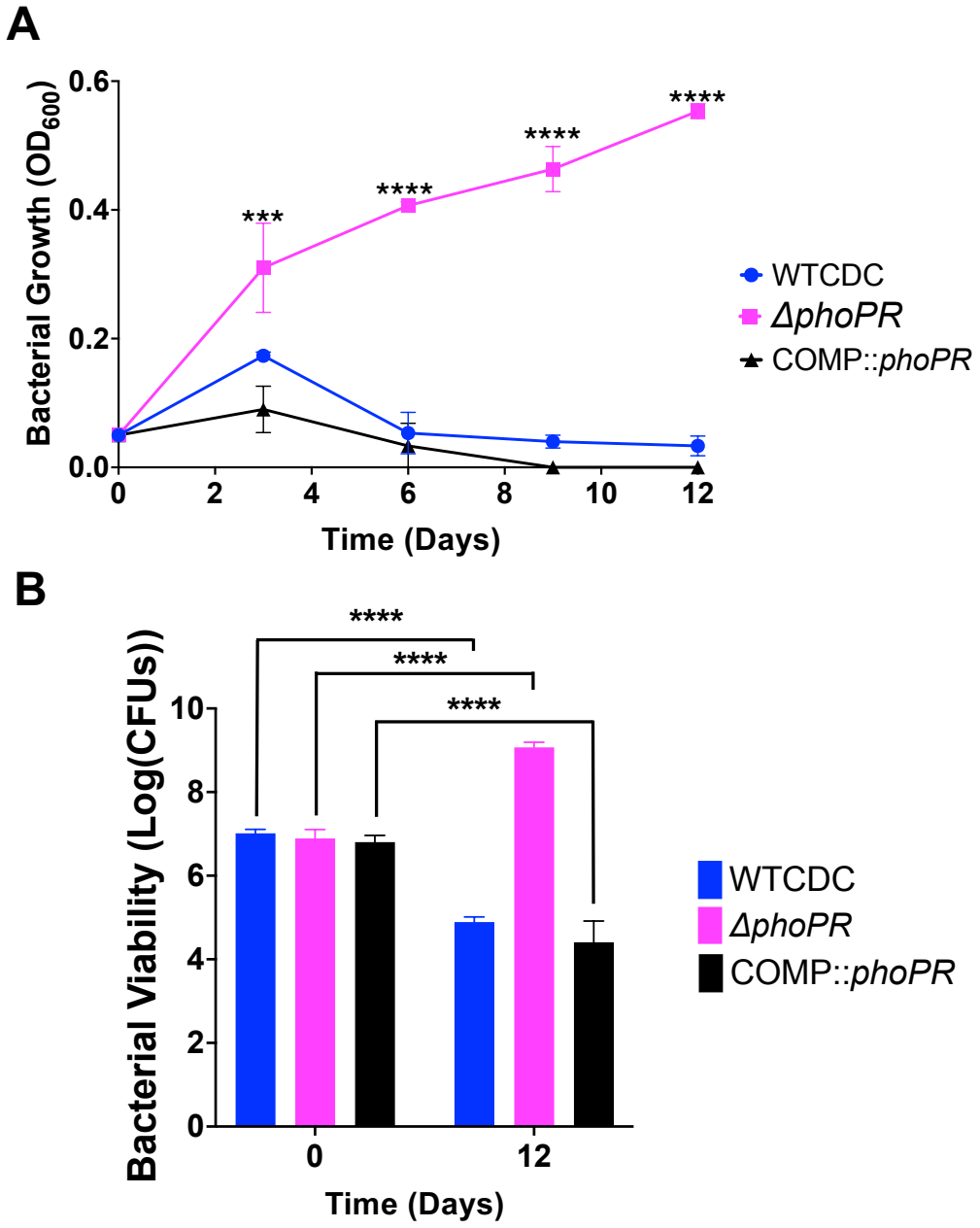
A
Bacterial Growth (OD600)
0.6
0.4
0.2
0.0
0
2
4
6
8
10
12
Time (Days)
***
****
****
****
WTCDC
ΔphoPR
COMP::phoPR
B
Bacterial Viability (Log(CFUs))
10
8
6
4
2
0
0
12
Time (Days)
****
****
****
WTCDC
ΔphoPR
COMP::phoPR

Figure 4

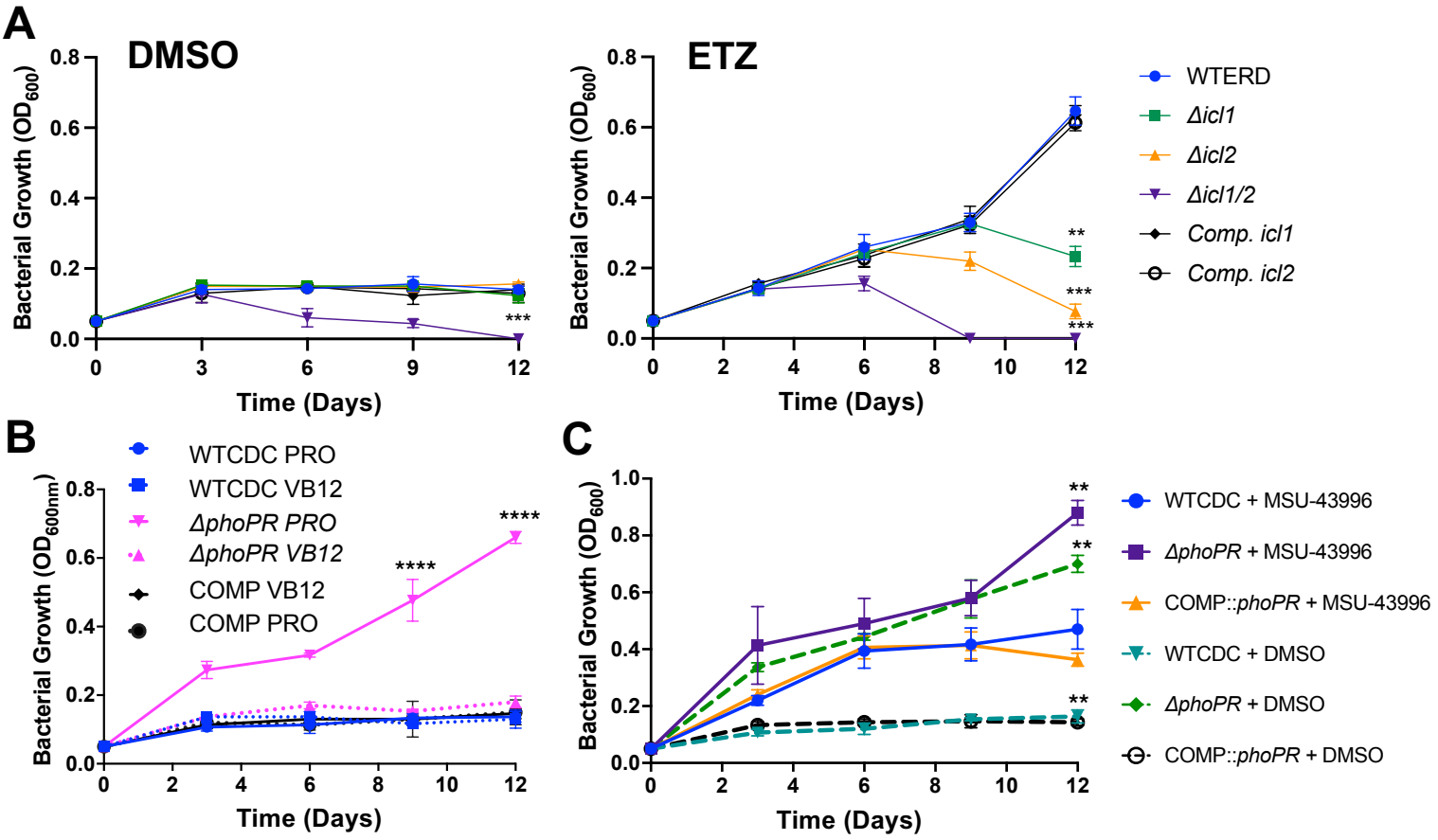
A
DMSO
ETZ
Bacterial Growth (OD600)
Time (Days)
WTERD
Δicl1
Δicl2
Δicl1/2
Comp. icl1
Comp. icl2
B
WTCDC PRO
WTCDC VB12
ΔphoPR PRO
ΔphoPR VB12
COMP VB12
COMP PRO
Bacterial Growth (OD600nm)
C
WTCDC + MSU-43996
ΔphoPR + MSU-43996
COMP::phoPR + MSU-43996
WTCDC + DMSO
ΔphoPR + DMSO
COMP::phoPR + DMSO

Figure 5

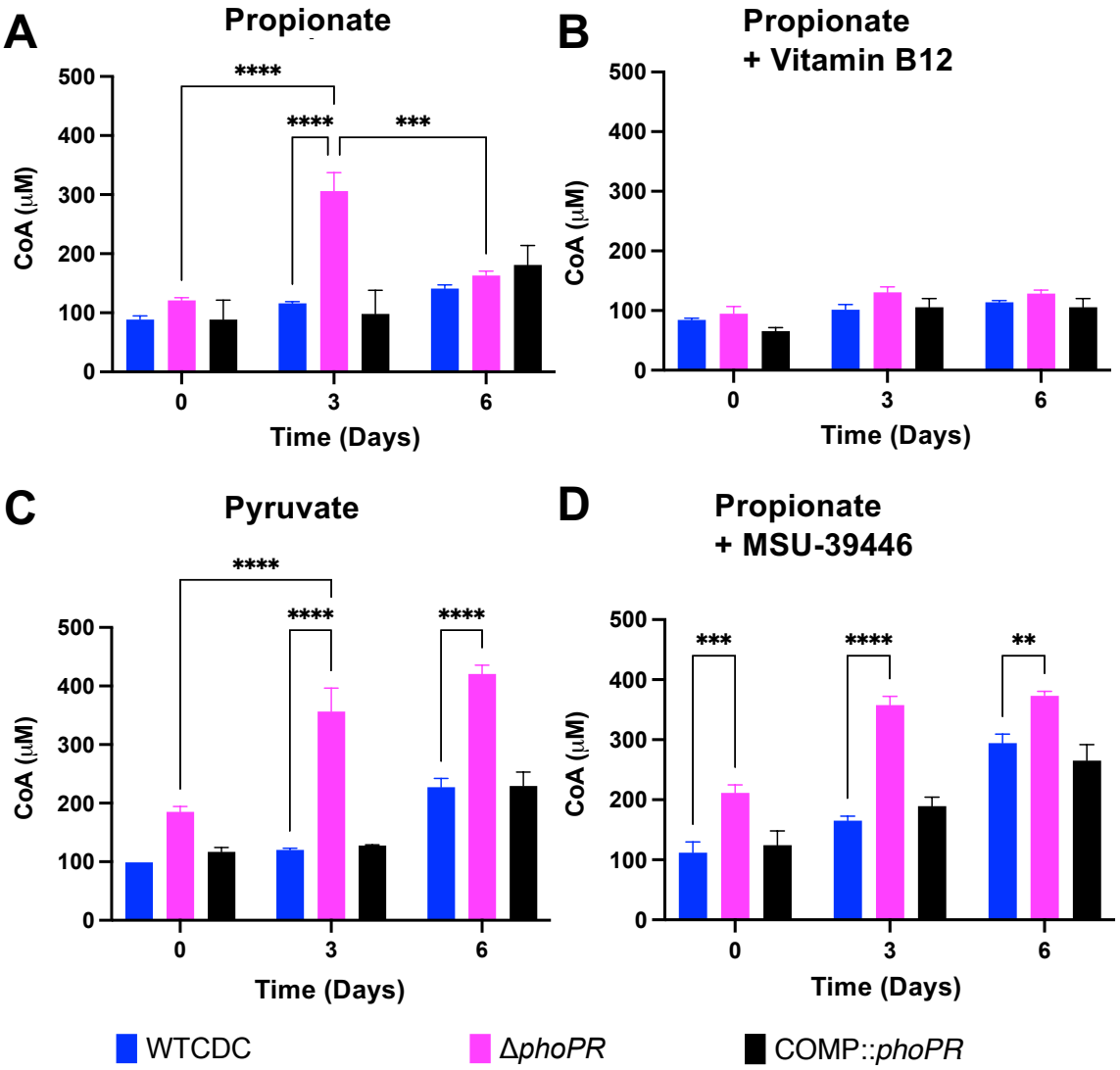
A
Propionate
B
Propionate
+ Vitamin B12
C
Pyruvate
D
Propionate
+ MSU-39446
CoA (μM)
Time (Days)
0
3
6
100
200
300
400
500
****
***
**
WTCDC
ΔphoPR
COMP::phoPR

Figure 6

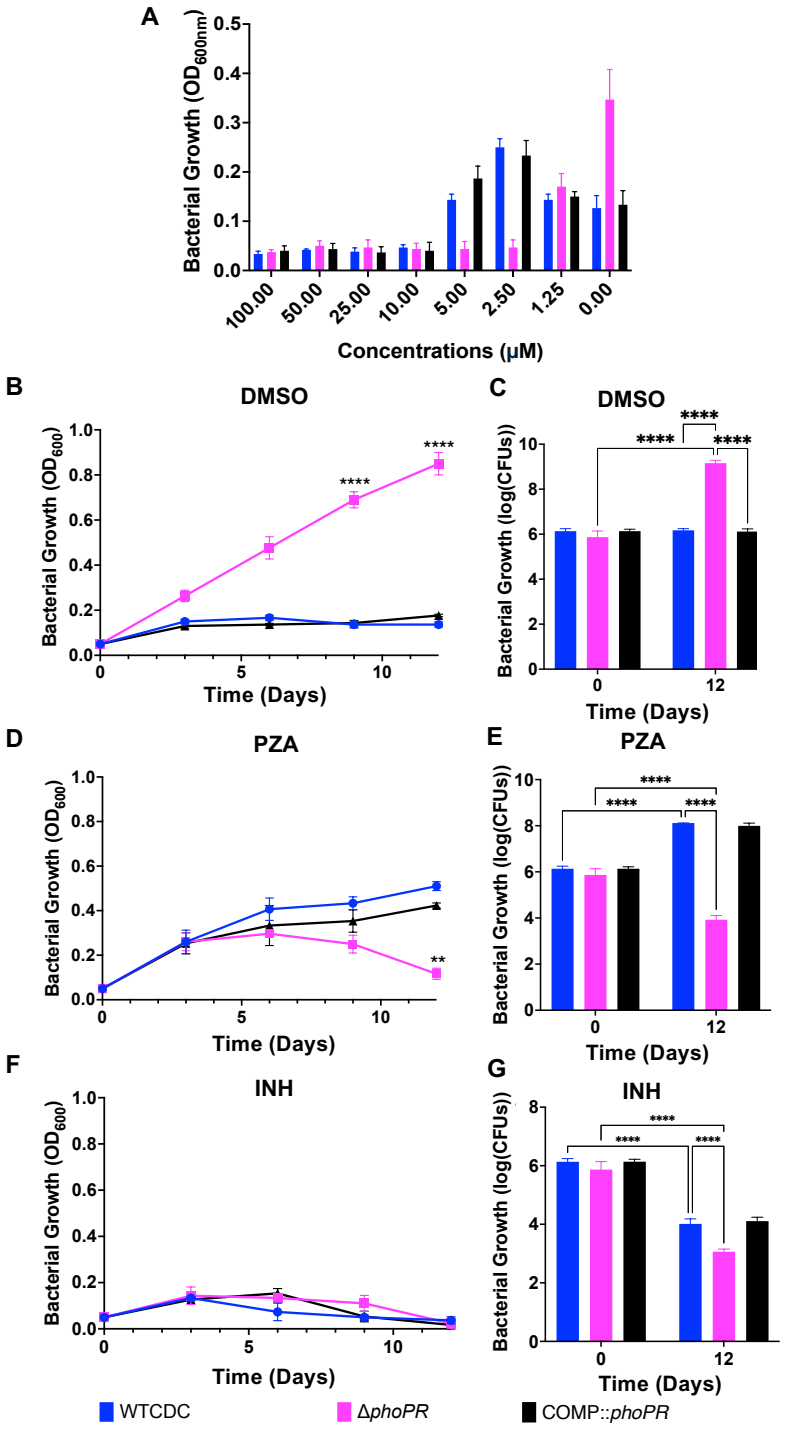
A
Bacterial Growth (OD600nm)
0.5
0.4
0.3
0.2
0.1
0.0
100.00
50.00
25.00
10.00
5.00
2.50
1.25
0.00
Concentrations (μM)
B
DMSO
Bacterial Growth (OD600)
1.0
0.8
0.6
0.4
0.2
0.0
****
****
0
5
10
Time (Days)
C
DMSO
Bacterial Growth (log(CFUs))
10
8
6
4
2
0
****
****
****
0
12
Time (Days)
D
PZA
Bacterial Growth (OD600)
1.0
0.8
0.6
0.4
0.2
0.0
**
0
5
10
Time (Days)
E
PZA
Bacterial Growth (log(CFUs))
10
8
6
4
2
0
****
****
****
0
12
Time (Days)
F
INH
Bacterial Growth (OD600)
1.0
0.8
0.6
0.4
0.2
0.0
0
5
10
Time (Days)
G
INH
Bacterial Growth (log(CFUs))
8
6
4
2
0
****
****
****
0
12
Time (Days)
WTCDC
ΔphoPR
COMP::phoPR

Figure 7

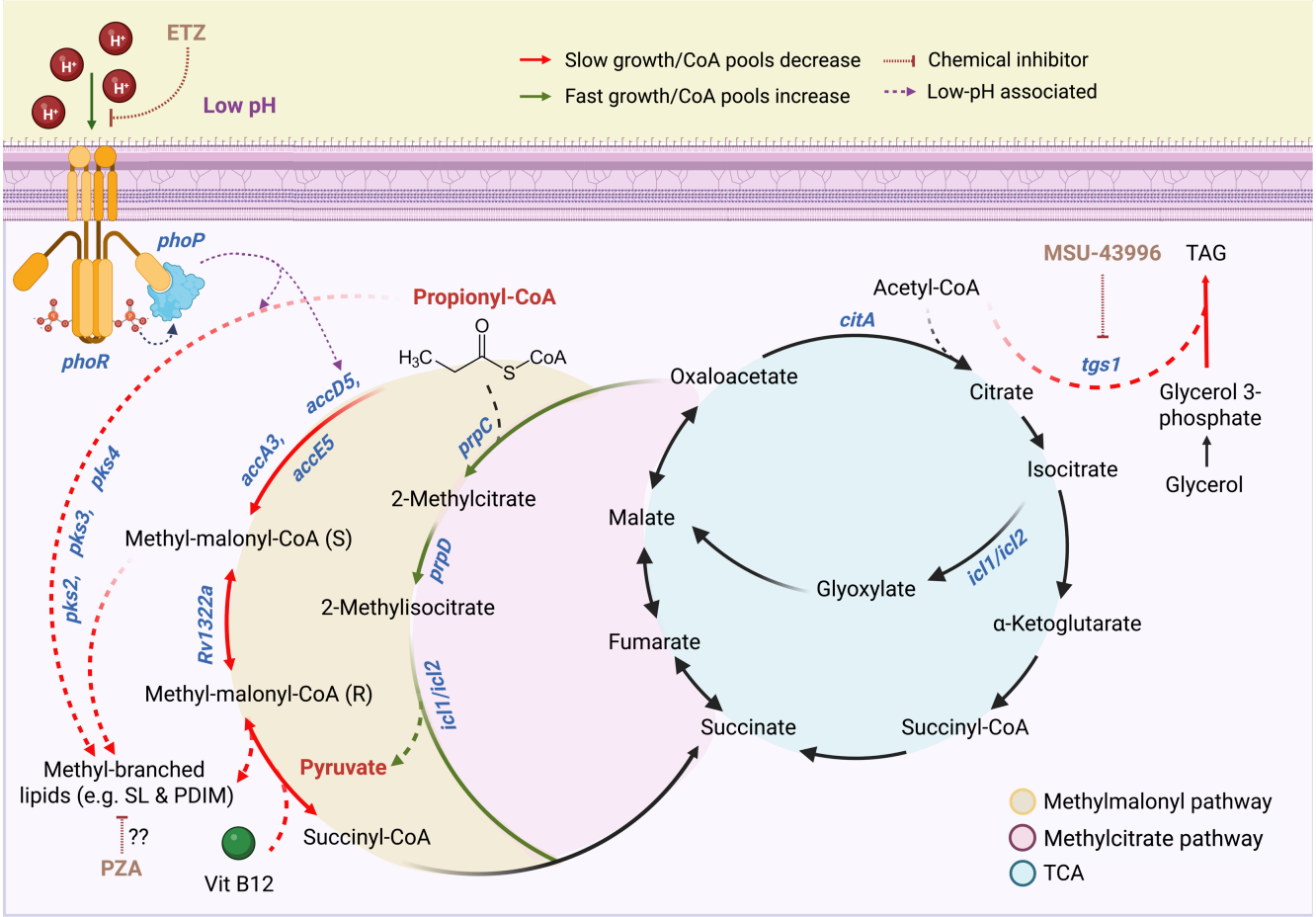
ETZ
Low pH
Slow growth/CoA pools decrease
Fast growth/CoA pools increase
Chemical inhibitor
Low-pH associated
phoP
phoR
Propionyl-CoA
MSU-43996
TAG
Acetyl-CoA
citA
tgs1
Glycerol 3-phosphate
Glycerol
Oxaloacetate
Citrate
Isocitrate
α-Ketoglutarate
Succinyl-CoA
Succinate
Fumarate
Malate
Glyoxylate
icl1/icl2
accD5,
accA3,
accE5
prpC
2-Methylcitrate
prpD
2-Methylisocitrate
Methyl-malonyl-CoA (S)
Rv1322a
Methyl-malonyl-CoA (R)
pks2, pks3, pks4
Methyl-branched lipids (e.g. SL & PDIM)
??
PZA
Vit B12
Pyruvate
Succinyl-CoA
Methylmalonyl pathway
Methylcitrate pathway
TCA

Figure 8

Supplemental Table and Figures

Mycobacterium tuberculosis growth arrest on propionate at acidic pH is suppressed by mutations in *phoPR* and pyrazinamide treatment

Heather M. Murdoch[1,2], Shelby J. Dechow[1,2], Bassel J. Abdalla[1] and Robert B. Abramovitch[1]

[1]Department of Microbiology, Genetics & Immunology, Michigan State University, East Lansing, MI,48824

[2]Co-first authors contributed equally to this study.

Supplemental Table

Table S1: Transposon Mutant Propionate Selection Summary

Supplemental Figure Legends

Figure S1. Bacterial Growth and viability of WT, Δ*phoPR* mutant, and complemented strains grown on propionate and treated with MSU-43996 at neutral pH. A) bacterial growth of the three strains on propionate at pH 7.0, showing no significant differences in growth rate. B) bacterial growth of the three strains on propionate at pH 7.0, treated with MSU-43996 or the vehicle, showing no major differences in growth rates based on strain or treatment.

Figure S2. PhoPR restricts growth at acidic pH by diverting carbon from the methyl citrate cycle. A) CFUs from the corresponding experiment in Figure 5A, showing cell death in the ETZ treated icl2 and icl1/2 knockouts. **B)** CFUs of Vitamin B12 treated Mtb strains. **C)** CFUs for figure 5C showing enhanced growth of MSU-43996 treated Mtb. Note, that timepoints are different, but CFUs are from the same experiment. **D**) Vitamin B12 does not impact the growth of strains at neutral pH. A one-way ANOVA was used for the viability experiments, * <0.05, ** <0.01, *** <0.001, **** <0.0001. Experiments were replicated at least twice with similar results.

Figure S3. Function of Icl and PhoPR at neutral pH on propionate. Growth of Mtb strains at pH 7.0 on propionate. ETZ did not impact growth in the *Icl1* or *Icl2* single mutants. The double icl1/2 mutant dies due to propionate toxicity. An unpaired t-test was used between individual groups for the growth curves, * <0.05, ** <0.01, *** <0.001, **** <0.0001. Experiments were replicated at least twice with similar results.

Figure S4. Itaconic acid inhibits enhanced growth of the Δ*phoPR* mutant. Itaconic acid inhibits the ability of the Δ*phoPR* to grow on propionate at pH 5.7. An unpaired t-test was used between individual groups for the growth curves, * <0.05, ** <0.01, *** <0.001, **** <0.0001. Experiments were replicated at least twice with similar results.

Figure S5. Free CoA pools on glycerol as a sole carbon source. During acid growth arrest on glycerol, all three strains maintain relatively low free CoA pools. Two-way ANOVA was used for this analysis, * <0.05, ** <0.01, *** <0.001, **** <0.0001. Experiments were replicated at least twice with similar results.

Figure S6. Vitamin B12 inhibits enhanced growth of WT Mtb treated with PZA. The inhibition of enhanced growth is consistent with PZA inhibiting lipid synthesis to promote growth, as making another lipid synthesis pathway available abolishes enhanced growth. Multiple comparison unpaired t-test was used for the analysis between treatments and the control, and between strains receiving the same treatment, * <0.05, ** <0.01, *** <0.001, **** <0.0001. Experiments were replicated at least twice with similar results.

Figure S7. Vitamin B12 inhibits enhanced growth of WT Mtb treated with PZA. CFU data for OD data presented in Figure S6.

Figure S8. Sensitivity of Mtb to PZA on Pyruvate as a sole carbon source at pH 5.7. PZA treatment does not result in enhanced growth with pyruvate as a sole carbon source.

Figure S9. PZA suppresses acid growth arrest on propionate in Mtb Erdman. To determine if the enhanced growth by PZA is conserved across strains, the PZA treatment experiment from Figure 7 which as conducted in CDC1551, was repeated in Mtb Erdman. Multiple comparison Unpaired t-tests were used for the growth assays, and one-way ANOVA was used for the viability assays, * <0.05, ** <0.01, *** <0.001, **** <0.0001. Experiments were replicated at least twice with similar results.

Figure S10. Sensitivity of Mtb to PZA treatment at pH 7.0. Control experiment for data in Figure 7, showing PZA is not active on Mtb grown in propionate at pH 7.0.

Table S1: Transposon Mutant Propionate Selection Summary

Mutant #	Approx AT or TA site/gene length (nt)	MT number	Rv Number	Gene Number	PDIM Mutation?	Fold Change (Day 14/Day0)
1.1	416/1458	MT0783	Rv0758	*phoR*	None	3.5
1.2	159/1458	MT0783	Rv0758	*phoR*	None	3.3
1.4	311/744	MT0782	Rv0757	*phoP*	None	1.5
2.1	278/1458	MT0783	Rv0758	*phoR*	*ppsE*	2.1
2.4	145/1458	MT0783	Rv0758	*phoR*	*ppsE*	1.9
3.2	145/1458	MT0783	Rv0758	*phoR*	*ppsE*	1.8
3.3	1124/1458	MT0783	Rv0758	*phoR*	*ppsE*	3.6
3.4	416/1458	MT0783	Rv0758	*phoR*	*ppsE*	1.8
4.1	378/1458	MT0783	Rv0758	*phoR*	*ppsE*	1.7
4.2	378/1458	MT0783	Rv0758	*phoR*	*ppsE*	3.5
4.3	416/1458	MT0783	Rv0758	*phoR*	*ppsE*	2.1
4.4	416/1458	MT0783	Rv0758	*phoR*	*ppsE*	2.2

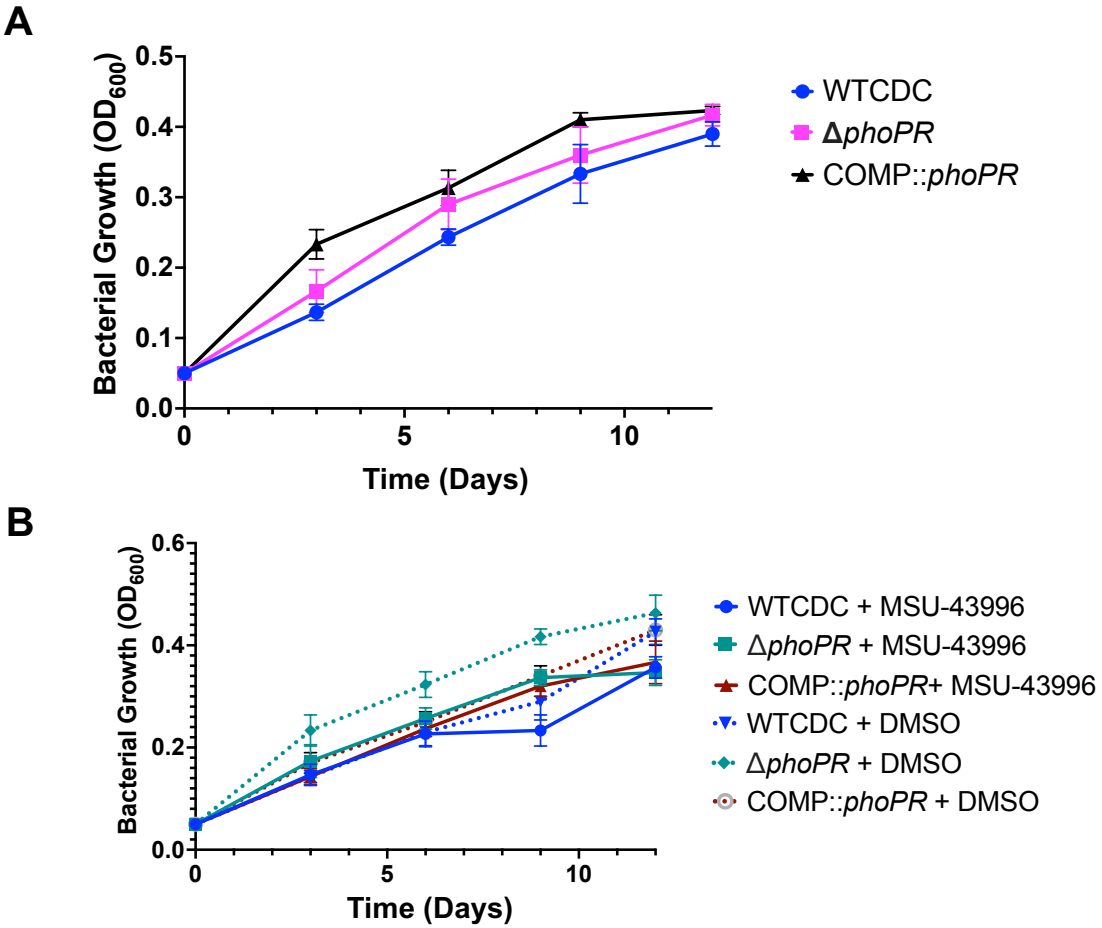

Supplementary Figure 1

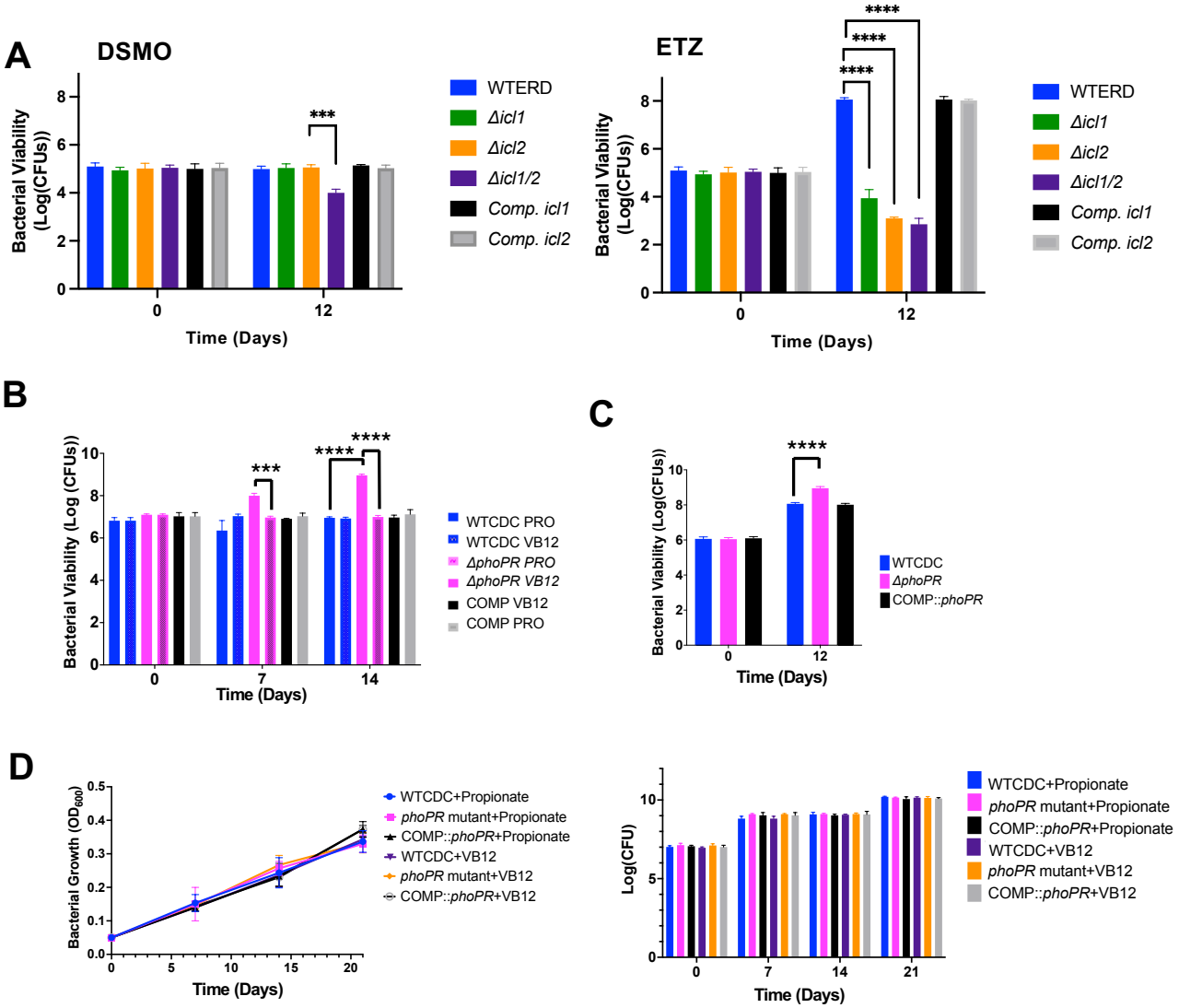

Supplementary Figure 2

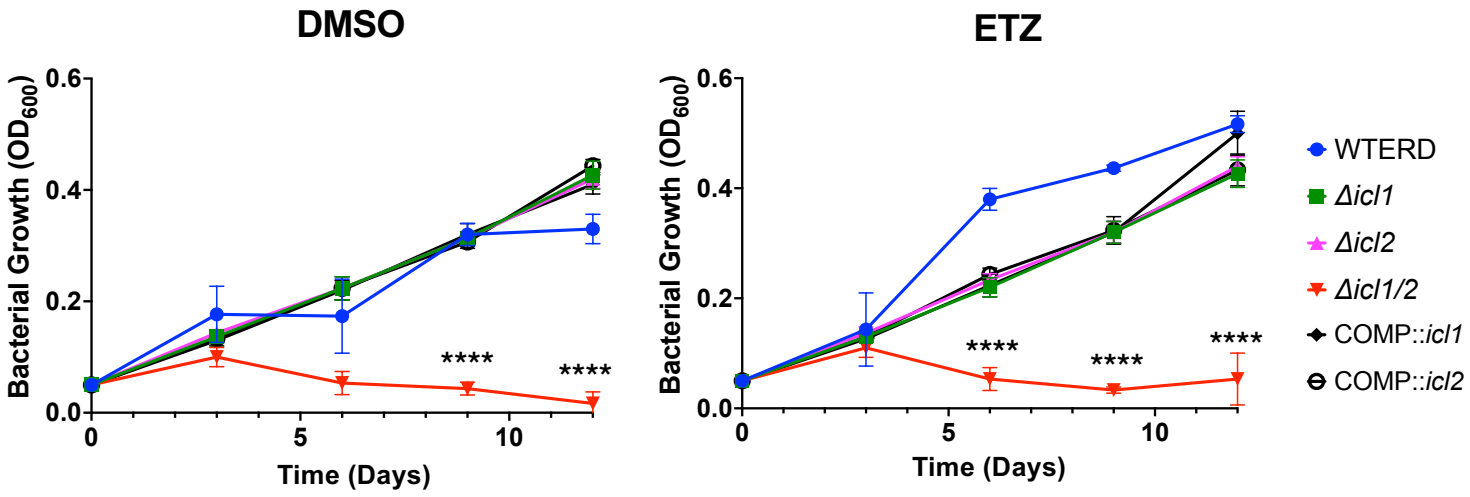

Supplementary Figure 3

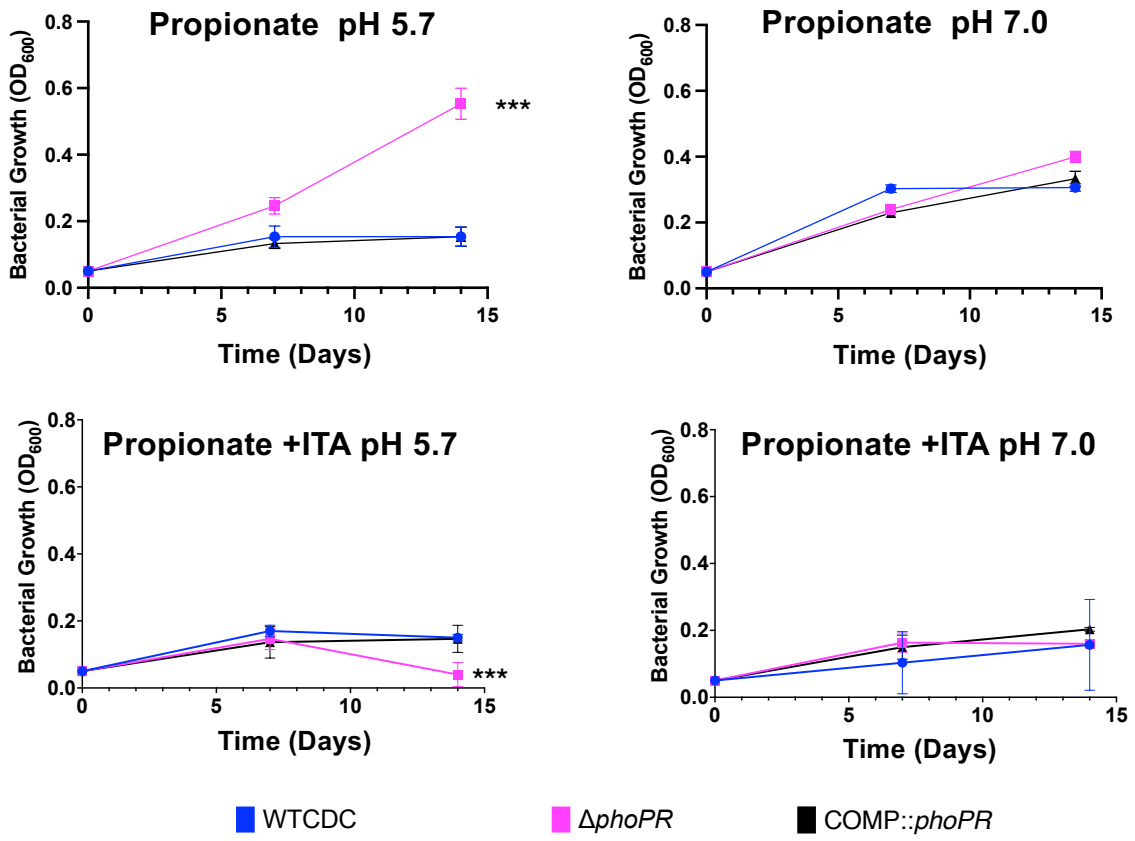

Supplementary Figure 4

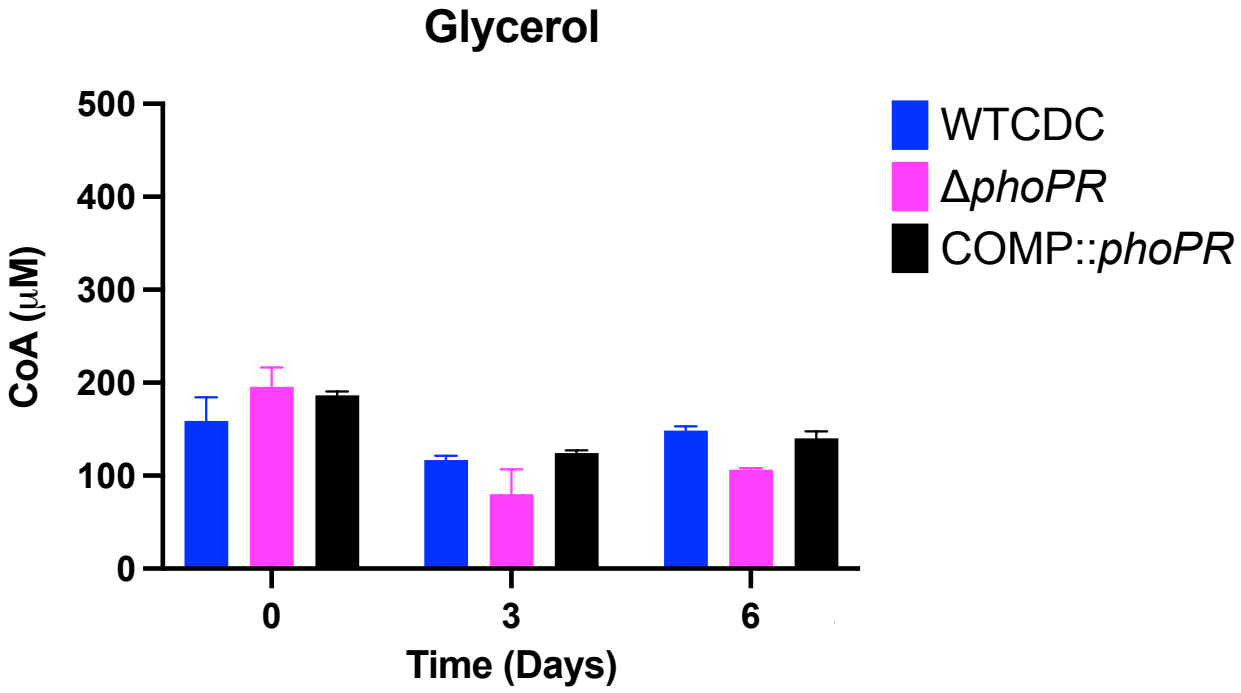

Supplementary Figure 5

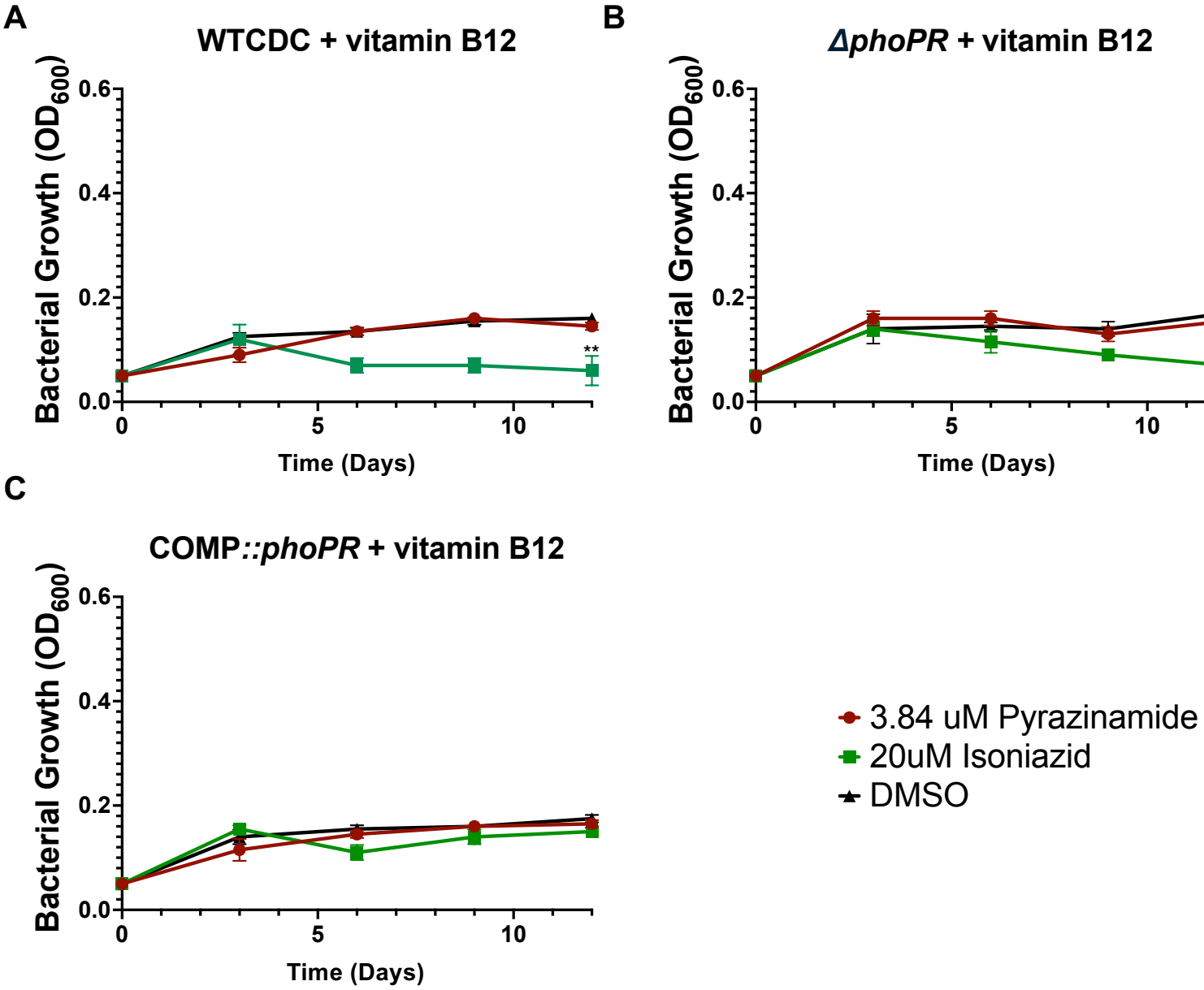

Supplementary Figure 6

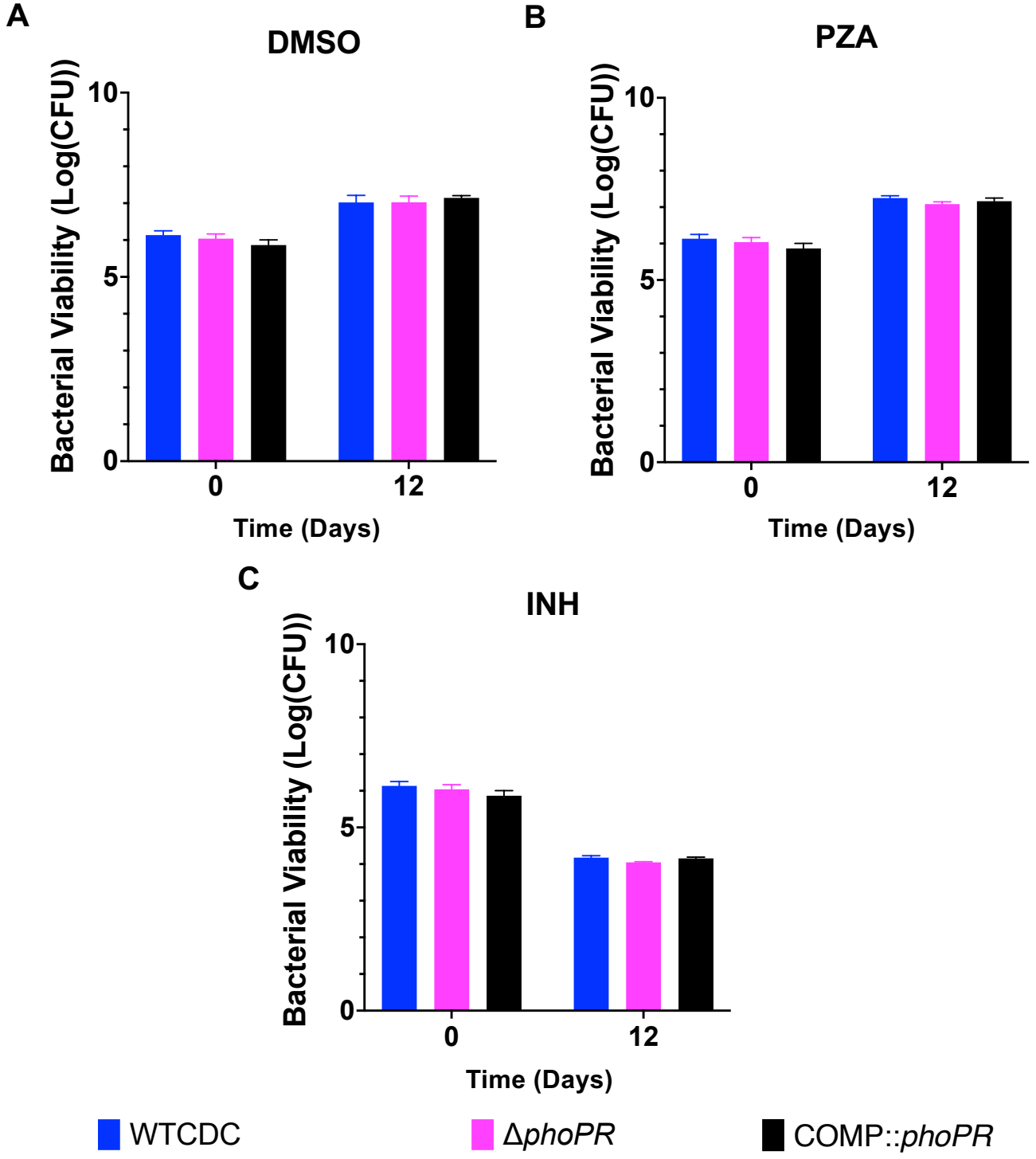

Supplementary Figure 7

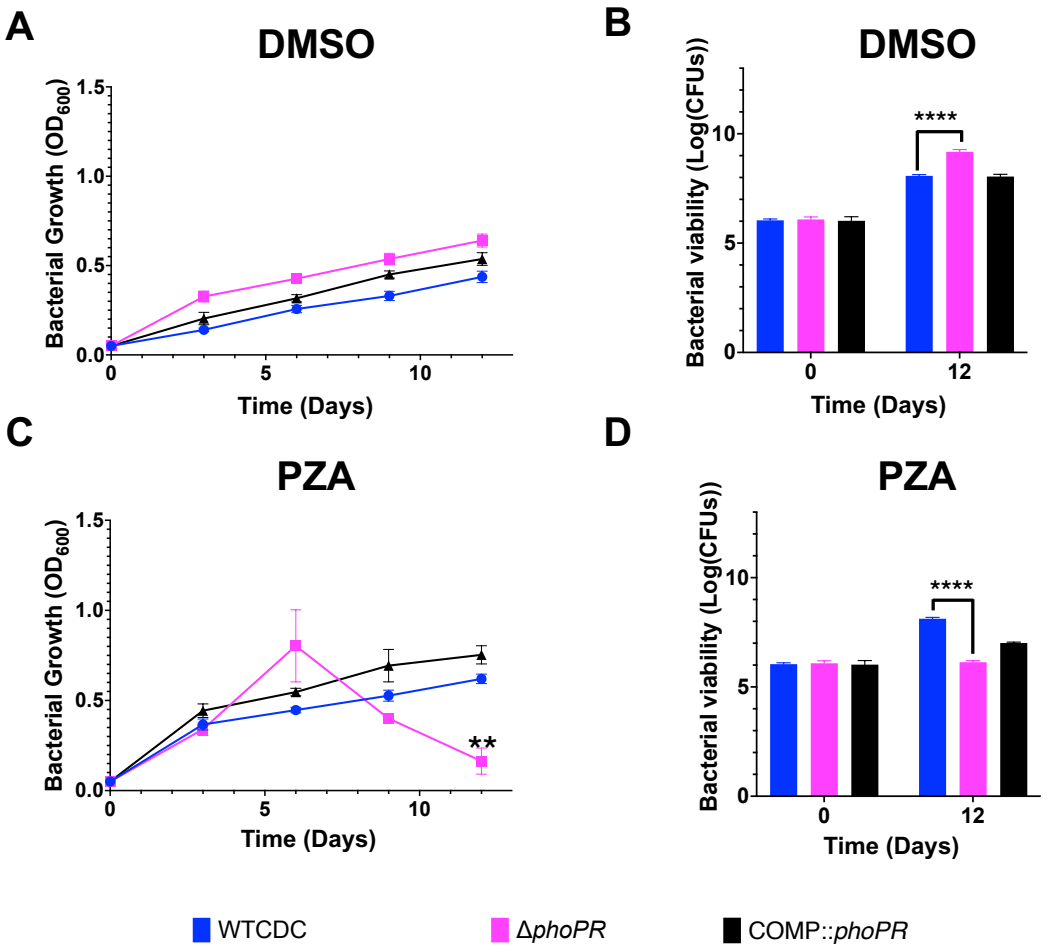

Supplementary Figure 8

A

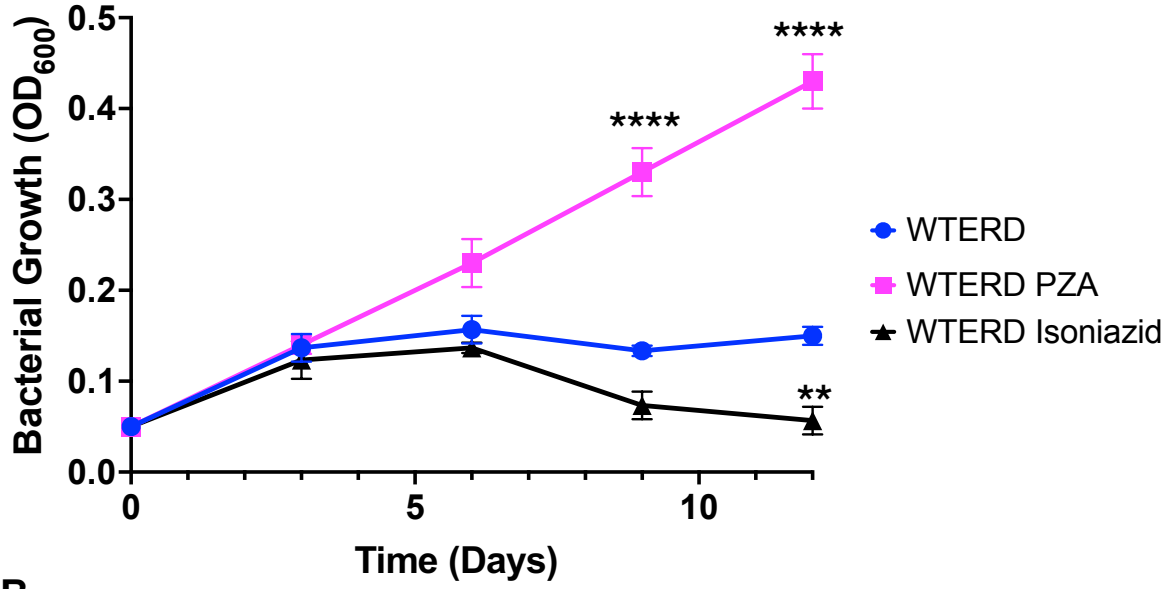

B

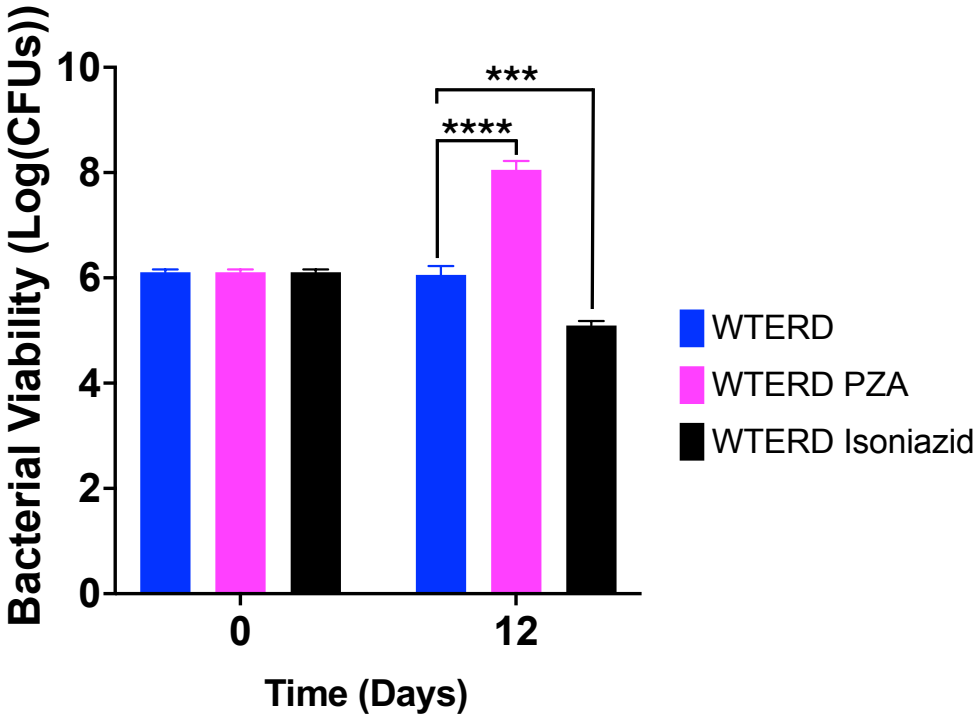

Supplementary Figure 9

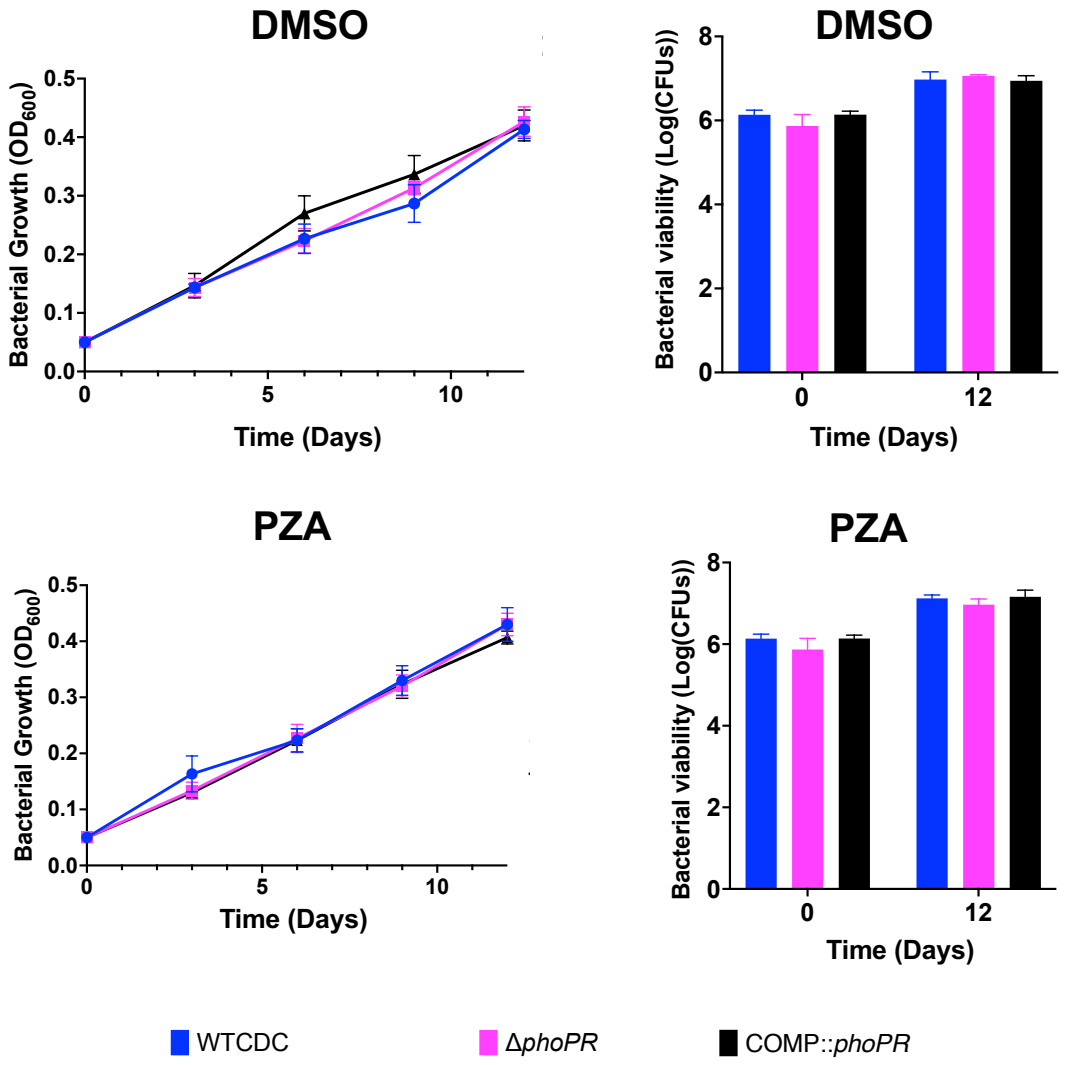

Supplementary Figure 10